# LOCAL WEAKENINGS OF FRAUNHOFER LINES ON THE SOLAR DISK

by

Gary Allen Chapman

---

A Dissertation Submitted to the Faculty of the

DEPARTMENT OF ASTRONOMY

In Partial Fulfillment of the Requirements
For the Degree of

DOCTOR OF PHILOSOPHY

In the Graduate College

THE UNIVERSITY OF ARIZONA

1968

THE UNIVERSITY OF ARIZONA

GRADUATE COLLEGE

I hereby recommend that this dissertation prepared under my direction by **Gary Allen Chapman**

entitled **Local Weakenings of Fraunhofer Lines on the Solar Disk**

be accepted as fulfilling the dissertation requirement of the degree of **Doctor of Philosophy**

Neil R. Sheeley, Jr. — Dissertation Director — May 2, 1968 — Date

After inspection of the final copy of the dissertation, the following members of the Final Examination Committee concur in its approval and recommend its acceptance:*

| | |
|---|---|
| T. L. Swihart | May 3, 1968 |
| Ray Weymann | May 3, 1968 |
| Donald J. Taylor | May 3, 1968 |
| Bart J. Bok | May 3, 1968 |
| R. F. Hilliard | May 27, 1968 |

*This approval and acceptance is contingent on the candidate's adequate performance and defense of this dissertation at the final oral examination. The inclusion of this sheet bound into the library copy of the dissertation is evidence of satisfactory performance at the final examination.

STATEMENT BY AUTHOR

This dissertation has been submitted in partial fulfillment of the requirements for an advanced degree at The University of Arizona and is deposited in the University Library to be made available to borrowers under rules of the Library.

Brief quotations from this dissertation are allowable without special permission, provided that accurate acknowledgment of the source is made. Requests for permission for extended quotation from or reproduction of this manuscript in whole or in part may be granted by the head of the major department or the Dean of the Graduate College when in his judgment the proposed use of the material is in the interests of scholarship. In all other instances, however, permission must be obtained from the author.

SIGNED: Gary A. Chapman

## ACKNOWLEDGMENTS

I gratefully acknowledge the advice and encouragement of Dr. B.J. Bok and Dr. R.J. Weymann of the Steward Observatory.

I am indebted to many members of the staff of the Solar Division of Kitt Peak National Observatory for their good-natured help, most notably:

Dr. James Brault and Mr. Charles Slaughter, especially, for supplying computer programs used in this investigation and helping with their operation,

Mr. David Chapman for help in certain aspects of observing,

Dr. A.K. Pierce for his generosity and congeniality,

and most of all, Dr. Neil Sheeley for his guidance, great help, and encouragement as advisor for this dissertation.

Acknowledgment is also made for help given by the staff of the photographic lab, particularly Mr. John Lutnes, and Mr. Mark Hanna; and to the staff of the computer lab, particularly Mr. Myron Gross and Miss Ann Cramblett.

Interesting conversations were also had with Mr. F.H. Chaffee, Dr. W.C. Livingston, and N. Alexander.

I especially wish to thank my wife, Joy, for her faith, patience, and help in typing and checking the dissertation.

TABLE OF CONTENTS

LIST OF ILLUSTRATIONS

Page

LIST OF TABLES

ABSTRACT

Previous studies have shown that certain Fraunhofer lines are appreciably weakened in small regions having high magnetic field strength not associated with sunspots. The weakenings, which quite often appear as gaps in lines on spectrograms, form a delicate photospheric network on spectroheliograms, similar to, but finer than, the familiar chromospheric Ca II $K_{232}$ network. The photospheric network seen in the $\lambda$6302.5 line of Fe I has a typical contrast of about 25-35% for regions in the vicinity of the disk center. This network is cospatial with the photospheric magnetic field seen on Leighton-type Z-photos, whereas the K network is not cospatial with the photospheric magnetic field but often extends beyond the boundaries defined by the photospheric field.

Fraunhofer lines are weakened partly by magnetic splitting of their Zeeman components. However, if one predicts the amount of weakening from Zeeman splitting, knowing the shape of the intensity profile of the line and the strength of the magnetic field, one finds that direct Zeeman

splitting is a minor cause of line weakening, at least for lines of neutral atoms. The importance of non-Zeeman effects is demonstrated by the appearance of weakenings in magnetically-insensitive lines. Furthermore, lines of ionized atoms are weakened appreciably less than lines of neutral atoms; and lines arising from levels having high excitation potential tend to be weakened less than lines arising from low excitation levels thus indicating that higher degrees of excitation and ionization prevail in these magnetic field regions. This higher degree of excitation and ionization suggests that in the line-forming layers of the photosphere, the temperature is higher in magnetic field regions than elsewhere, a conclusion given some support by observations showing that white light faculae, which are in all probability cospatial with magnetic field regions, have higher temperatures than the surrounding photosphere. Observations by others in the UV continuum also show brighter-than-average features in magnetic field regions.

Thus photospheric magnetic fields of several hundred gauss correspond to regions of altered physical conditions seen as white-light faculae near the solar limb and as the photospheric network in the line-forming regions.

# I. INTRODUCTION

Solar magnetic fields were first measured by Hale in sunspots in 1908. Although sunspots have the strongest fields observed on the sun, with typical field strengths of two to three kilogauss, Hale (1922) found that there were strong magnetic fields having strengths of a few hundred gauss not directly associated with sunspots. Unlike sunspots, no manifestation of these fields could be seen in white light; consequently, these regions were called "invisible spots" by Hale. Leighton (1959), on his early Zeeman photographs (Z-photos), found fields of 100-200 gauss away from spots but in plage regions. He also found that Ca II K-emission on spectroheliograms was fairly well, but not perfectly, correlated in position with magnetic fields on Z-photos and appeared whenever the field strength exceeded his threshold sensitivity of approximately 20 gauss. Sheeley (1964), on his Z-photos, found field strengths of several hundred gauss for small regions (less than 3000 kilometers across) sometimes far removed from sunspots. Later, in an attempt to confirm these

observations of strong fields using the Mt. Wilson Observatory magnetograph, Harvey and Sheeley (1965) found non-spot fields exceeding 200 gauss in active regions.

Such strong fields might be expected to alter the strength and shape of magnetically sensitive Fraunhofer lines by separating their Zeeman components. Sheeley (1967) found, on spectrograms, that where small-scale magnetic fields of several hundred gauss occurred, certain Fraunhofer lines were appreciably weakened, the weakenings appearing as "gaps" in the lines. Their one-dimensional size was found to vary from several thousand kilometers down to the resolution limit of a few hundred kilometers. Not all lines were affected the same amount; those lines having greater magnetic sensitivity often seemed to be more affected. However, the weakening of Fraunhofer lines cannot be due entirely to Zeeman effects since the magnetically insensitive line, $\lambda$5123.7 A of Fe I, was also found to weaken in a magnetic field. These same regions also showed strong CaII $K_{232}$ emission. Beckers and Schröter (1966) found similar features (in the magnetically sensitive $\lambda$6173 line of Fe I) which they called magnetic knots. These features, which were not pores, had magnetic field

strengths, determined directly from Zeeman splitting, of hundreds of gauss. The corresponding central intensities of the line were increased by about 30-35%.

Thus magnetic fields do cause weakening of Fraunhofer lines but not entirely because of magnetic splitting. It is not difficult to suppose that the physical conditions in the line-forming regions of the solar atmosphere are affected by the presence of the magnetic field. Very little is known about the two-dimensional nature of weakenings nor is their exact relationship to magnetic fields well understood. The purpose of this dissertation is to study the weakenings of selected Fraunhofer lines in order to determine how they are correlated in position and strength with magnetic fields and to define the dominant processes that produce them.

The following types of observations have been used to determine the properties of weakenings: First, spectroheliograms have been made in highly Zeeman-sensitive lines in order to determine the two-dimensional nature of weakenings. Second, in order to determine the strength and spatial distribution of magnetic fields for comparison with spectroheliograms of weakenings, Z-photos of the same

region were also made. Third, the fact that chromospheric lines (such as the CaII K-line) and the weaker photospheric lines show qualitatively different "local brightenings" suggests that such "local brightenings" may depend on the height in the solar atmosphere at which the line is formed. To investigate this aspect of weakenings without the interference of Zeeman splitting, spectroheliograms were made in magnetically-insensitive lines of various strength.

Fourth, the direct influence of the magnetic field on a Fraunhofer line was investigated by:

(1) taking two spectroheliograms simultaneously, one in a magnetically-insensitive line and the other in a magnetically-sensitive line, and

(2) taking spectroheliograms sequentially in lines of greatly differing Zeeman sensitivity but similar central intensity and equivalent width.

Fifth, wavelength dependence (within a Fraunhofer line) of weakenings was investigated in two dimensions by making step-scan spectroheliograms in which the same region is repeatedly photographed while the bandpass of the spectroheliograph is stepped, in wavelength, through the center of the spectrum line from one picture to the next. Sixth,

intensity profiles of selected lines were obtained from a few of the best spectrograms available. The behavior of the intensity profile in and out of these magnetic field regions not only provided information in itself but also gave confirmation, in a general way, to some of the results obtained with the spectroheliograph.

## II. OBSERVATIONS

### A. Selection of Fraunhofer Lines

In order to determine the direct effects of magnetic fields, a number of Fraunhofer lines of widely different Zeeman sensitivity were selected subject to the condition that they also be suitable for taking spectroheliograms. Whenever possible, lines having simple Zeeman triplet patterns were used to simplify the analysis of Zeeman splitting. To determine the influence of non-Zeeman effects, lines having a large variation in equivalent width, central intensity, and excitation potential both for neutral and singly ionized atoms were chosen. Certain practical effects such as scattered light in the spectroheliograph, meant that lines which were too weak (less than about 40 mA equivalent width) or too shallow (central intensity greater than about 70% of the continuum) could not ordinarily be used for making spectroheliograms. Magnetically-insensitive lines are important because, having no Zeeman splitting, they permit the direct study of non-Zeeman effects. However, there are not very many of these lines, and although a systematic

search was made for them using the Moore multiplet table and the Utrecht atlas of solar lines, only eight were found that were well suited for use with the spectroheliograph. A summary of the more important lines used with the spectroheliograph is contained in Table 1.

## B. Equipment and Technique

The spectroheliograms and spectrograms used in this dissertation were made with the McMath Solar Telescope, which has a focal length of approximately 300 feet and an image scale of 2.3 seconds of arc per millimeter.

The spectroheliograph contains a 15-foot Czerny-Turner spectrograph whose only refractive optical component is a curvature correction lens beneath the entrance slit. There are two exit slits, individually adjustable, which produce two monochromatic images of the sun having a wavelength difference that is easily adjustable from 0 to about 35 A. The exit slit illuminates a 9-1/2 inch long strip on an 8 x 10 inch photographic plate while scanning across the plate thus producing the spectroheliogram. A typical scanning speed for an ordinary spectroheliogram (such as shown in Figure 1) using I-F emulsion was approximately 20 sec/cm

Table 1

Data for More Important Fraunhofer Lines

Used with Spectroheliograph

| λ(A) | El. | EP(eV) | W(mA) | CI | "g"$\lambda^2$ |
|---|---|---|---|---|---|
| 4855.7 | 687 Fe I | 3.37 | 60 | 0.44 | 3.5 |
| 4863.6 | 687 Fe I | 3.43 | 48 | 0.43 | 0.0 |
| 5123.7 | 16 Fe I | 1.01 | 101 | 0.32 | 0.0 |
| 5131.5 | 66 Fe I | 2.21 | 72 | 0.40 | 6.2 |
| 5250.2 | 1 Fe I | 0.12 | 62 | 0.39 | 7.5 |
| 5264.8 | 48 Fe II | 3.33 | 45 | 0.58 | 2.3 |
| 5409.8 | 18 Cr I | 1.03 | 154 | 0.25 | 3.6 |
| 5434.5 | 15 Fe I | 1.01 | 184 | 0.24 | 0.0 |
| 5576.1 | 686 Fe I | 3.43 | 113 | 0.38 | 0.0 |
| 5691.5 | 1087 Fe I | 4.30 | 38 | 0.67 | 0.0 |
| 6240.6 | 64 Fe I | 2.21 | 40 | 0.68 | 3.9 |
| 6247.6 | 74 Fe II | 3.87 | 49 | 0.68 | 4.3 |
| 6302.5 | 816 Fe I | 3.67 | 83 | 0.53 | 9.9 |

with a bandpass of 25 mA. The dispersion of the spectroheliograph was approximately 0.8 A/mm at λ5200.

The 45-foot spectrograph is also of the Czerny-Turner design. The entrance slit used was approximately 4 inches long and 100 microns wide. The photographic plates were usually I-F emulsion, 4 x 10 inches. Exposure times were typically 0.2-0.5 seconds near λ5000 with a dispersion of 0.14 A/mm. Some uncalibrated spectrograms, taken during exceptionally good seeing in July and September, 1966, by N. Sheeley, have been calibrated and used in this investigation.

Observing Procedures: The observing procedure for the spectroheliograph was different than that for the spectrograph and will be discussed first. At the beginning of the observing day, a region of interest on the sun was chosen either by looking at the sun in Hα through a Zeiss filter or by looking at the main image in white light. The purpose of this quick search was to find those areas most likely to have a large amount of magnetic flux outside of sunspots. Having positioned the desired region near the entrance slit, the exit slit was set on the appropriate part of the spectrum line by eye since no line-finding

photometer was then available. Since no automatic guiding or positioning device was available either, sunspots were generally used to reposition the image after each exposure. In order to obtain wavelength information and to have one picture in the center of the Fraunhofer line, a number of separate exposures were usually made on each 8 x 10 inch plate of the same area on the sun. Typically, these exposures ran for 3 cm each (allowing 5 such pictures on a plate) and were separated in wavelength usually by about 25 mA. In order to determine exactly what part of a spectrum line was being used, a short calibration scan was produced, usually at the beginning and end of the spectroheliogram, in which the wavelength passing through the spectroheliograph was continuously changed. At known wavelength intervals, the observer's arm quickly passed over the entrance slit thus producing streaks in an expanded line profile at known wavelength intervals. The intensity on most spectroheliograms was calibrated by placing a Kodak Step Tablet over the entrance slit during the second short calibration scan (expanded line profile).

Since the spectrograph slit covers such a small area on the solar disk, some care must be used in

positioning this slit so as to include magnetic field regions (gaps) on the spectrogram. Since magnetic field regions cannot be seen in white light, a λ6302.5 spectroheliogram was taken of an active region. The magnetic field regions, appearing as locally-bright features, could then be selected for spectrograms. After selecting the desired spectral region and sometimes optimizing the position of the entrance slit by looking, in the photographic port, for strong gaps in the line, a plate was loaded and, at a moment of good seeing, exposed. After a number of spectrograms were obtained, a calibration plate was produced by placing a Kodak Step Tablet on the entrance slit and exposing the plate several times longer than for a normal spectrogram. Development of all plates was in full-strength HC-110 for 7 minutes at a temperature of approximately 20° C.

## C. Reduction Procedures

The transmissions of selected features on both spectrograms and spectroheliograms have been measured with a Boller and Chivens microphotometer. The analyzing beam of the microphotometer, which was formed by an adjustable slit near the light source, usually had a length on the plate of 0.4 mm corresponding to approximately 700 km on

the sun. Transmission measurements for spectroheliograms were usually recorded by a Speedomax paper chart recorder. The transmissions of the selected features and the proper background were taken from the paper chart and converted into relative intensities by means of the calibration curve in graph form. Then, for each selected feature, $(I_f/I_b) - 1 = \Delta I/I$ was determined, where f refers to the feature and b refers to the background.

Spectrograms were handled differently. The transmission of the spectrogram was sampled at about 20$\mu$ intervals in the direction of dispersion. The measurements were then filtered (to remove high-frequency noise), digitized, and recorded on magnetic tape. These transmission measurements were converted into an intensity plot in a two-step procedure using the Kitt Peak CDC 3200 computer. First, the transmissions were converted to relative intensities (using a program created by Charles Slaughter of Kitt Peak) and stored on magnetic tape. Second, the data from this magnetic tape was read into the computer, noise in the data was reduced and the smoothed intensities were plotted on a Cal Comp Digital Plotter, by means of a program created by James Brault of Kitt Peak.

Zeeman photographs were calibrated in a manner similar to that of Leighton (1959) in which a transmission profile of the average photosphere, obtained from a calibration scan on the Z-photo, was used to obtain $\frac{d \log T}{d \lambda}$. For many Z-photos using the Ca I λ6103 line, $\frac{d \log T}{d \lambda}$ had a value of 6-7 $A^{-1}$. The transmissions of the fields, T, and the background, $T_0$, on the Z-photo are converted to $\log \frac{T}{T_0}$ = $\Delta \log T$, which then gives the wavelength shift due to the Zeeman effect through $\Delta\lambda = \Delta \log T \left( \frac{d \log T}{d \lambda} \right)^{-1}$. The Zeeman shift, $\Delta\lambda$, is then converted into field strength knowing the magnetic sensitivity, $\Delta\lambda/B$, of the line. For the doubly-cancelled Z-photo shown in Figure 4(a) the calibration is $B_{\parallel} = 944 \log \frac{T}{T_0}$ gauss.

The error in $B_{\parallel}$, arising from the photographic cancellation process and noise, was about ±50 gauss (rms) for typical Z-photos of moderately good quality. The minimum discernible signal, determined from measurements of the noise in several Z-photos, was ±30 gauss (rms).

The error in $\Delta I/I$ from spectroheliograms depends on plate noise, the determination of the background intensity, and the calibration of the plate. Based upon experimental determinations of the first two, errors in $\Delta I/I$ are about

±5-10% of the measured value. Based upon uncertainties in the calibration curve, calibration errors are probably less than 5% of the measured value. Thus, the uncertainty in $\Delta I/I$ from spectroheliograms is approximately 10-15% of the measured value.

# III. RESULTS

## A. Two-Dimensional Characteristics

Weakenings occur on the sun in many forms and sizes from isolated points with a characteristic size of 700 km (1 arc-second) to nets or plages having rather complicated shapes. Figure 1, a spectroheliogram made in the λ6302.5 line of Fe I during very good seeing, will be used to show several aspects of weakenings. This spectroheliogram consists of five short scans (or pictures) which were made at slightly different wavelengths, starting in the line center and stepping to the violet. The picture on the left, which was taken in the center of the line, shows the weakenings best. A number of locally-bright regions can be found, especially near the large sunspot, that have a characteristic size of about 700 km. These regions correspond to a weakening of the line at its center of about 0.20-0.30. It is difficult to define the edges of larger features unambiguously. However, there are weakenings as large as 2100 km which have only moderate interior variations in intensity. Much larger regions have more complicated

Figure 1. λ6302.5 Spectroheliogram

This is a spectroheliogram from September 13, 1967 made in the λ6302.5 line of Fe I during very good seeing. The outermost narrow strips are calibration scans through the line. The largest of the five pictures is in the center of the line and the remaining four are to the violet as follows:

| Picture | Δλ (A) |
|---|---|
| 1 | 0.00 |
| 2 | -.02 |
| 3 | -.04 |
| 4 | -.06 |
| 5 | -.08 |

The largest of the five or six pores, seen in the fifth picture east of the large spot, is visible in every picture including the first. The penumbra of the large sunspot in Picture 1 has bright regions, adjacent to the umbra, which, in some sunspots, form bright rings around the umbra. These bright regions are not noticeable in Picture 5.

Approximate orientation:

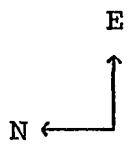

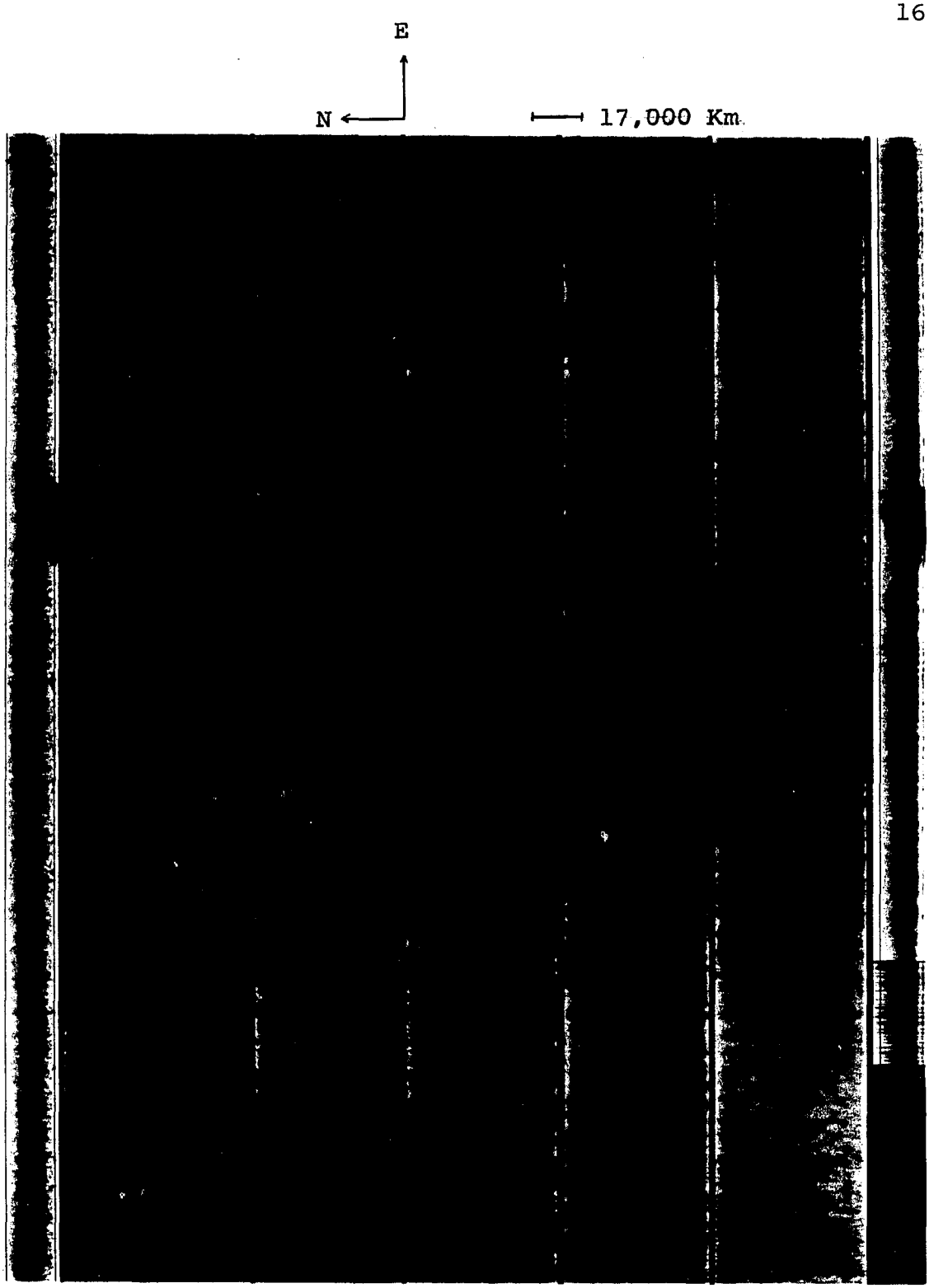


Fig. 1. λ6302.5

two-dimensional structure such as the large plage region just east of the large sunspot in Figure 1. The intensity of the interior of this plage has many local minima, appearing qualitatively as holes, thus giving the plage a "Swiss-cheese-like" appearance. In the long feature extending southwest from this plage, one can trace along a wiggly path for several ten-thousand kilometers in a generally northeast-southwest direction before a definite edge is encountered. It would thus appear that, within the resolution limitations imposed, weakenings can be continuous over rather long (up to $3 \times 10^4$ km) distances yet possess considerable two-dimensional fine structure.

The amount of weakening of various features in Figure 1 was found to be typically in the range 0.25-0.35 but exceeded 0.45 for some features, for example, brighter parts of the feature 21,000 km west of the large sunspot.

Photospheric weakenings, produced in "photospheric" lines, have smaller area and finer detail than corresponding chromospheric weakenings produced in "chromospheric" lines. (For our purposes, chromospheric weakenings are those that bear resemblance to weakenings seen in the cores of strong lines such as Ca I 4227, whose core is probably

formed in the chromosphere. Photospheric weakenings, which have a finer appearance than chromospheric weakenings, are usually seen in lines, such as λ6302.5, whose centers are probably formed in the photosphere.) Spectroheliograms taken in the wings of strong, chromospheric lines show weakenings that appear in size and shape more like photospheric weakenings than chromospheric ones. Figure 2 shows spectroheliograms taken in the λ6302.5 line and two strong lines whose centers may be formed in the chromosphere. Although the seeing was not as good as in Figure 1, the weakenings in λ6302.5 and the wings ($\Delta\lambda$ = -.18A and -.27A) of λ5183.6 have a sharper, finer two-dimensional appearance than the appearance of the weakenings in the center of λ5269.5 and λ5183.6, whose "fuzzier" appearance is somewhat like that of the chromospheric network. Thus, on a large scale, photospheric weakenings occupy approximately the same locations on the solar disk as do chromospheric weakenings, but the latter seem to "overflow" the boundaries defined by the photospheric weakenings. The different appearance of photospheric and chromospheric weakenings is shown more strikingly in Figure 3. The local brightenings seen at $\Delta\lambda$ = -.20A and +.23A in Ca I 4227 are much

Figure 2. Spectroheliograms in λ6302.5, λ5269.5 and λ5183.6

These spectroheliograms show that weakenings have a "fuzzy" appearance when seen in the centers of strong lines (λ5269.5 and λ5183.6) and cover a larger area than weakenings seen in photospheric lines (such as λ6302.5) and the wings of strong lines (λ5183.6, $\Delta\lambda \approx .20$A). The larger-area network in the core of λ5183.6 and λ5269.5 bears some resemblance to the Ca II chromospheric network and is therefore referred to as a chromospheric network. Since the photospheric network is cospatial with the photospheric magnetic fields, the chromospheric network is not cospatial with the photospheric magnetic fields.

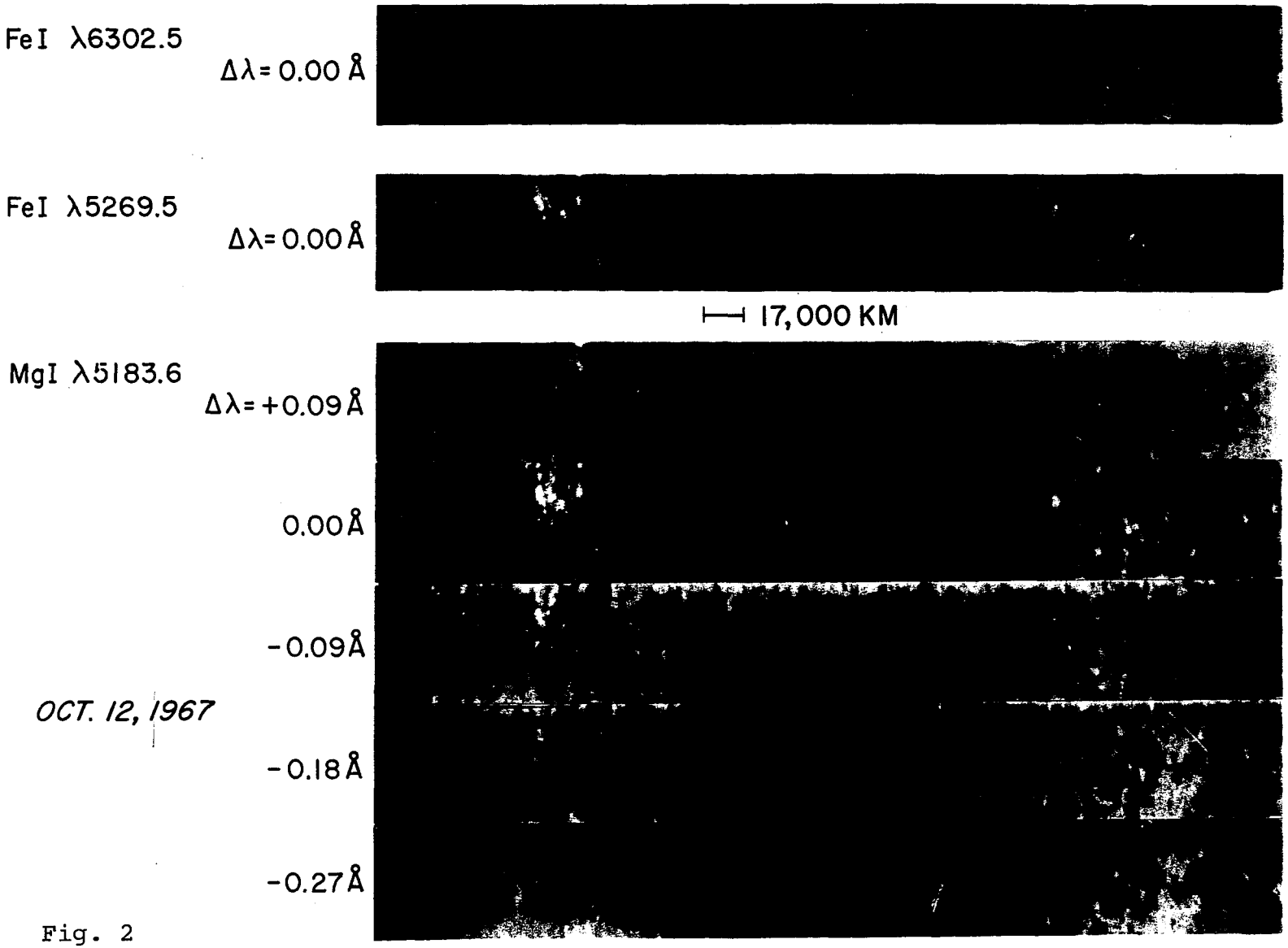
FeI λ6302.5
Δλ= 0.00 Å
FeI λ5269.5
Δλ= 0.00 Å
17,000 KM
MgI λ5183.6
Δλ= +0.09 Å
0.00 Å
-0.09 Å
OCT. 12, 1967
-0.18 Å
-0.27 Å

Fig. 2

Figure 3. Spectroheliograms in λ3934 and λ4227

These spectroheliograms also show that the chromospheric network, especially the $K_3$ chromospheric network, covers a larger area than the photospheric network (taken to be that seen in λ4227 at $\Delta\lambda \approx \pm .20$A). Since the photospheric magnetic field is cospatial with the photospheric network, the chromospheric network is not cospatial with the photospheric magnetic field.

Unlike the Ca II K-line, which has its greatest contrast in the core, the Ca I λ4227-line has greater contrast in the wings ($\Delta\lambda \approx \pm .20$A) than in the core.

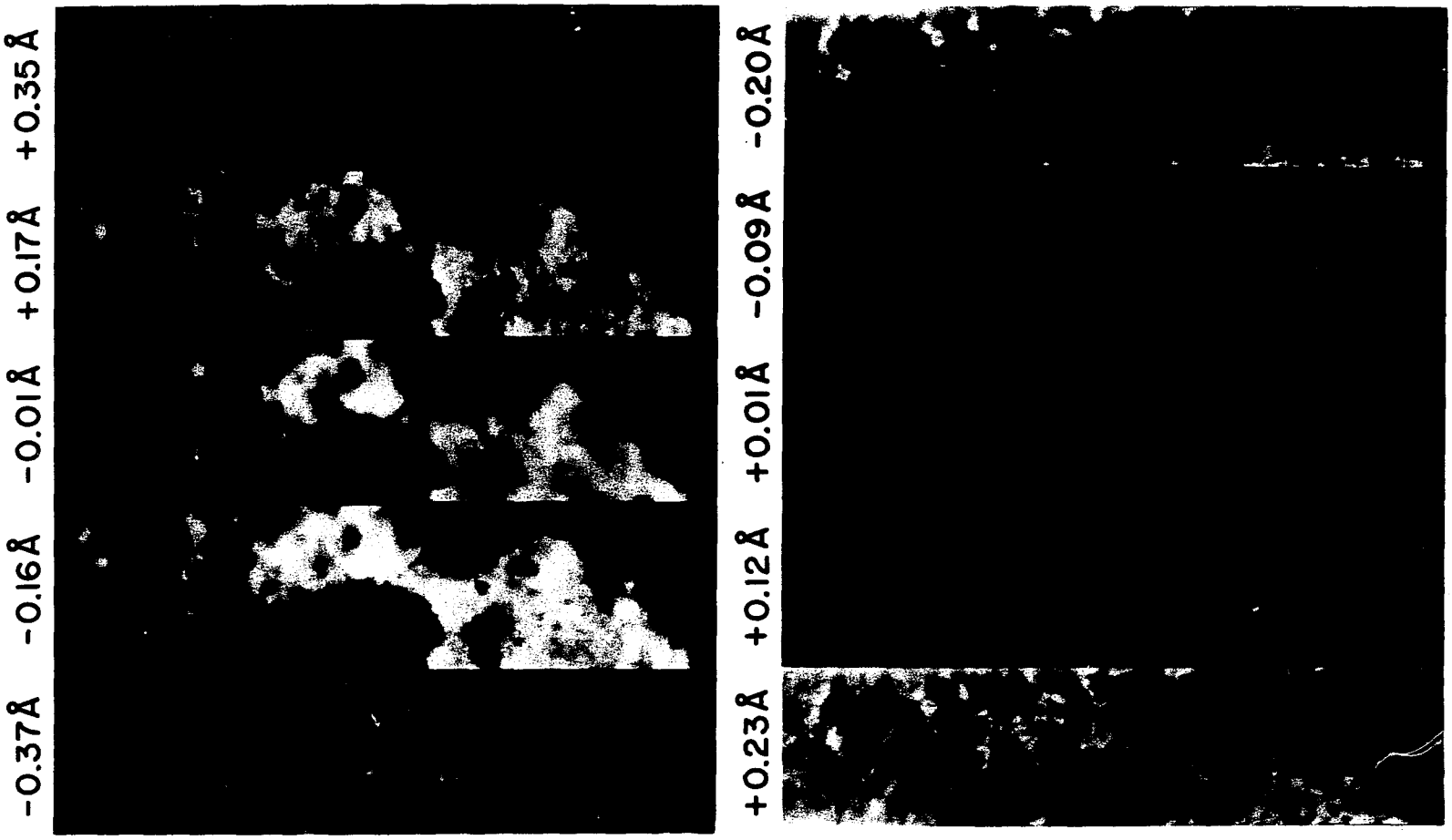
-0.37Å
-0.16Å
-0.01Å
+0.17Å
+0.35Å
+0.23Å
+0.12Å
+0.01Å
-0.09Å
-0.20Å
CaII λ3934
CaI λ4227
JANUARY 24, 1968
17,000 KM

Fig. 3

more delicate and finely structured than those seen in the core ($\Delta\lambda$ = +.01A). A somewhat similar situation is seen in the Ca II 3934 spectroheliogram in Figure 3. The bright network seen at $\Delta\lambda$ = +.35A and -.37A has a finer and more delicate two-dimensional structure than that seen in the core ($K_3$). The off-band ($\Delta\lambda \approx \pm$.35A) network, although more delicate than the $K_3$-network, is not as delicate as that in the wings of Ca I 4227, suggesting that one must go further into the wings of the K-line than .35A in order to see a network as finely detailed as that seen at $\Delta\lambda \approx$ 0.20A in the wings of Ca I 4227. Thus, weakenings, seen as locally-bright regions in the center of photospheric lines and in the wings of very strong chromospheric lines, form a photospheric network which is more delicate and covers less area than the familiar chromospheric network.

## B. Spatial Relationships with Fields

A major objective of this dissertation is to show the two-dimensional relationship between weakenings and $B_{\parallel}$, the line-of-sight magnetic field. A number of spectroheliograms and Z-photos have shown that photospheric weakenings coincide <u>exactly</u> with the photospheric line-of-sight

magnetic fields, in that wherever a line-of-sight magnetic field can be seen on Z-photos, a photospheric weakening will be found of the same size and shape. This close relationship will be illustrated by examining a spectroheliogram in a Zeeman-sensitive line and a Z-photo of the same region made within an hour or so as shown in Figure 4. Parts (a) and (b) of Figure 4 are Z-photos of the same region but of "opposite" polarity. (A field region of one polarity which appears brighter-than-average in (a) will appear darker-than-average in (b) and the reverse will be true for fields of the opposite polarity.) Part (c) of Figure 4 is a spectroheliogram in the highly Zeeman-sensitive line of Fe I at λ5131.5. Wherever there is a magnetic feature on the Z-photo there is usually a locally-bright region on the λ5131 spectroheliogram corresponding very closely to the shape and size of the field. Minor differences between the features on the two pictures are probably due chiefly to seeing and perhaps partly to the time difference between them.

Even more convincing evidence for the detailed spatial correspondence between photospheric magnetic fields and photospheric weakenings is shown in Figure 5. The

Figure 4. Z-photos and Spectroheliograms from August 13, 1967

Comparison of the Z-photo (a) and the λ5131 spectroheliogram (c) shows that wherever there is a magnetic field on the Z-photo, there is usually a locally-bright area on the λ5131 spectroheliogram of very nearly the same size and shape. Any differences are probably due chiefly to seeing and perhaps partly to time difference.

The λ5124 spectroheliogram (d), made simultaneously with (c), has locally-bright features appearing at the same places and having essentially the same size and shape as those on the λ5131 spectroheliogram, thus showing that magnetically-insensitive lines are also weakened in magnetic field regions.

The λ4855 spectroheliogram (e) shows that velocity-granules (granules that on spectrograms produce marked indentations on the red side of weak lines), appearing as small bright dots throughout most of the spectroheliogram, are modified in the magnetic field regions on the left side of the figure.

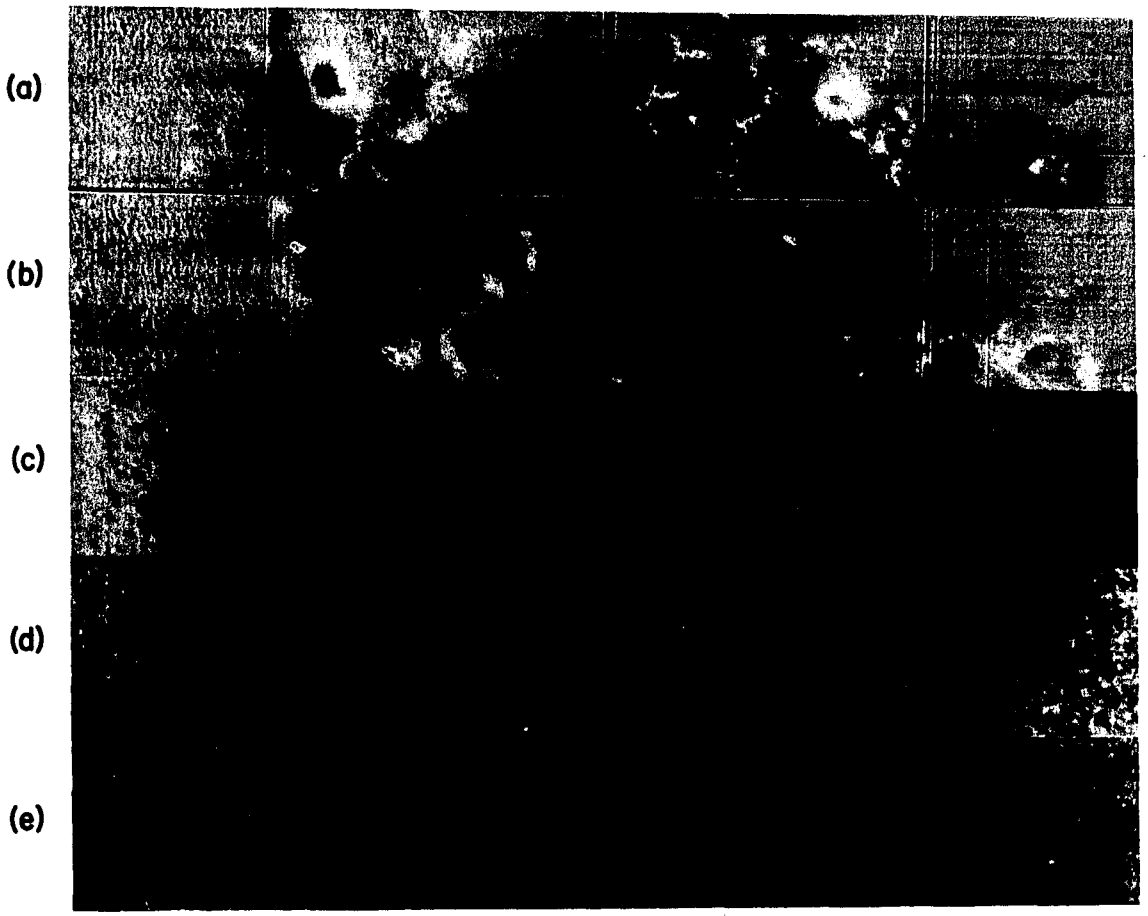


(a) Zeeman photograph $\lambda/4 = +$ (Ca I λ6103)

(b) Zeeman photograph $\lambda/4 = -$ (Ca I λ6103)

(c) Fe I λ5131 core $\left(\frac{\Delta\lambda}{B} = 3.1 \times 10^{-5}\ \text{Å/gauss}\right)$ } simultaneous

(d) Fe I λ5124 core $\left(\frac{\Delta\lambda}{B} = 0\right)$ } simultaneous

(e) Ni I λ4855 red wing $\left(\frac{\Delta\lambda}{B} = 1.6 \times 10^{-5}\ \text{Å/gauss}\right)$

Fig. 4. Z-photos and Spectroheliograms

Figure 5. Uncancelled and Cancelled Z-photos and λ6302.5 Spectroheliogram from September 13, 1967

The uncancelled Z-photos appearing in the upper-half of the figure show "polarized weakenings" which are alternately seen in slit 1 or slit 2 depending on the direction of the magnetic field (toward or away from the observer) in the weakening. These polarized weakenings are cospatial with the magnetic fields since they produce the magnetic field signal on the cancelled Z-photo. Furthermore, polarized weakenings corresponding to both polarities of the magnetic field, seen in the first picture of slit 1, are very similar in appearance to the weakenings seen in the ordinary λ6302.5 spectroheliogram. Therefore, photospheric weakenings are exactly cospatial with strong photospheric magnetic fields.

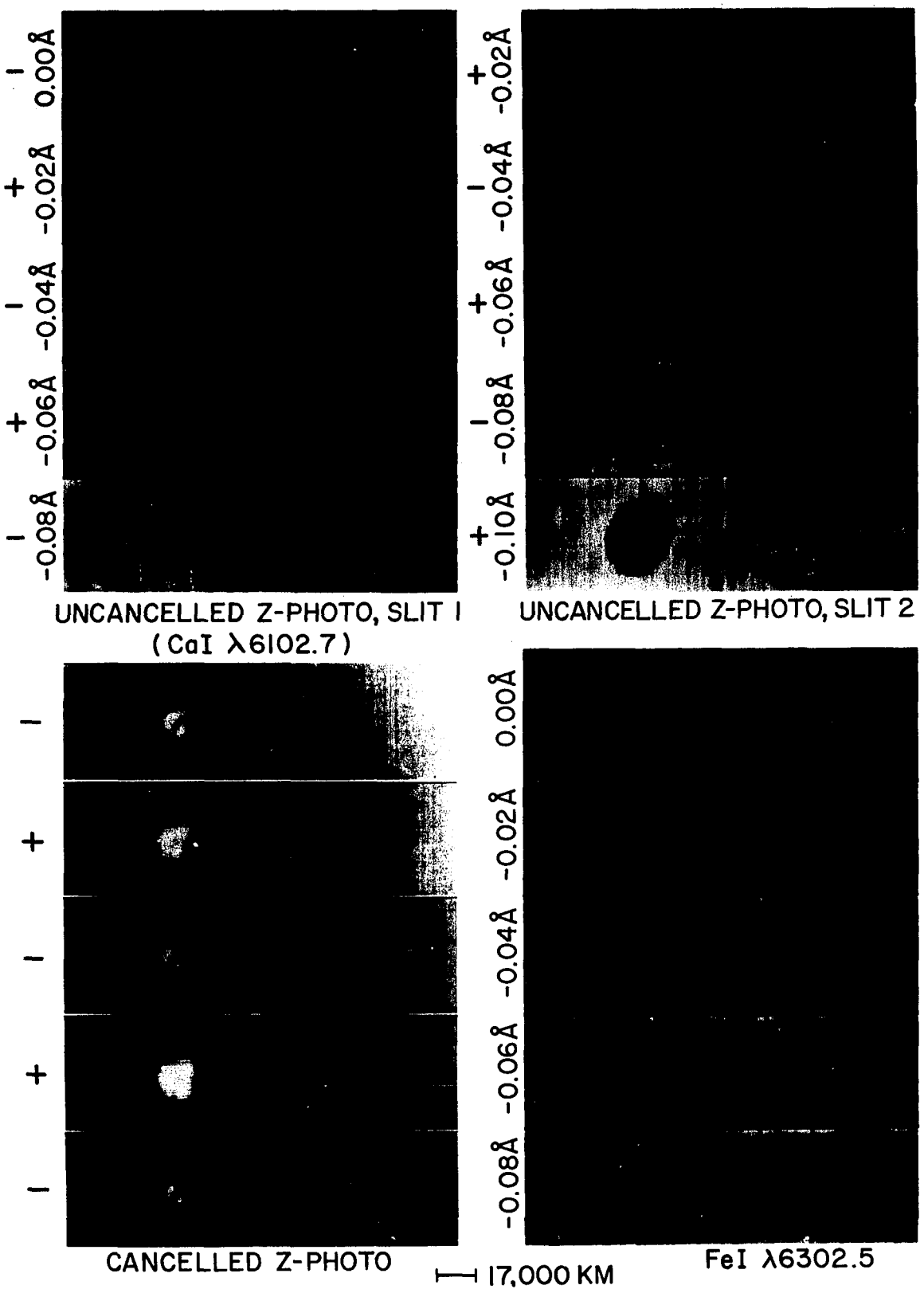


Fig. 5. Z-photos and Spectroheliogram

upper half of Figure 5 shows locally-bright features whose appearance on alternate frames of the spectroheliogram depends on the relation between the direction of the magnetic field (toward or away from the observer) and the orientation of the quarter-wave plate (optic axis inclined +45° or -45° with respect to the slit) over the entrance slit. Since the appearance of these features depends on the polarization of the light accepted for that frame or picture, they will be called "polarized weakenings" in analogy with the weakenings seen on ordinary spectroheliograms. As the polarity of the transmitted light is alternated from right-circular to left-circular between pictures, so the "polarized weakenings" appear and disappear in accordance with the direction of the field in them. This alternate appearance of the "polarized weakenings" is due to the spatial correlation between magnetic fields and photospheric line weakenings as shown in Figure 6. It is easy to see that when the uncancelled Z-photos in the upper half of Figure 5 are combined to produce the cancelled Z-photo in the lower left of Figure 5, the polarized weakenings produce the magnetic field signals on the Z-photo, showing that the polarized weakenings and magnetic fields coincide exactly.

Figure 6. "Polarized Weakenings" and Photospheric Brightness-Field Correlation

A line-of-sight magnetic field is directed toward the observer. Both exit slits of the spectroheliograph are on the violet side of the line. The exit slit that accepts left-circularly polarized light will see a low-contrast feature, L, for this field direction, whereas that exit slit that accepts right-circularly polarized light will see a high-contrast feature, R.

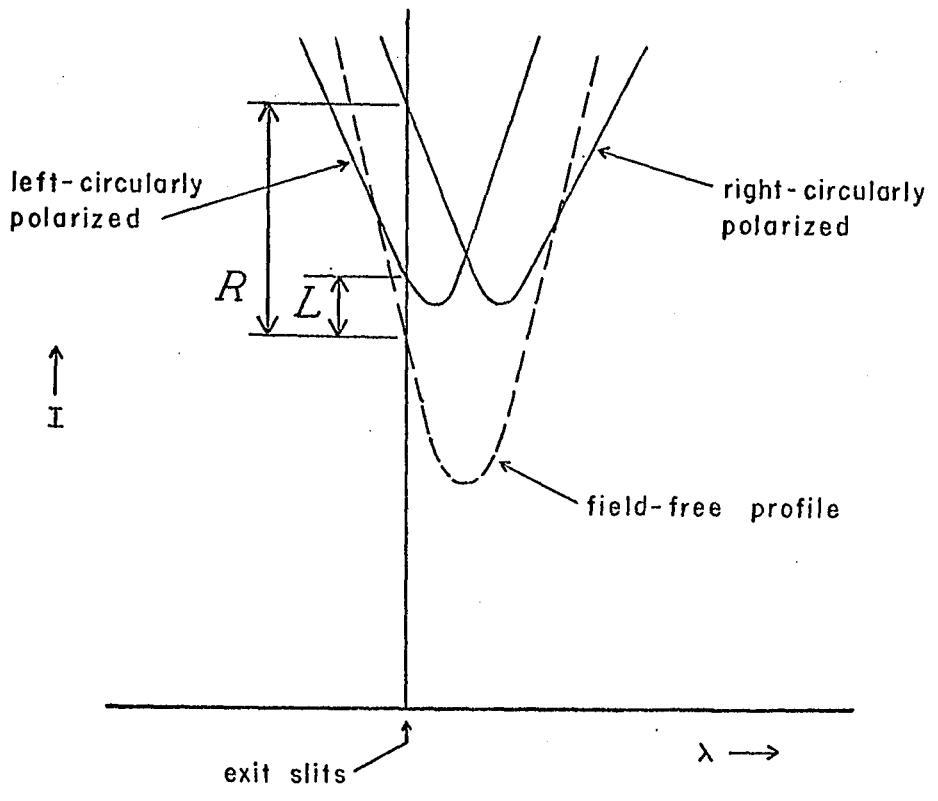


Figure 6. "Polarized Weakenings" and Photospheric Brightness-Field Correlation

Furthermore, the uncancelled Z-photo from slit 1 made in the center of the line shows weakenings of both polarities and looks very much like the ordinary λ6302.5 spectroheliogram. Slight differences are probably due to differences in seeing and perhaps partly to the time difference. Thus, we see that there is detailed spatial correspondence between photospheric magnetic fields and photospheric weakenings. A spectroheliogram made precisely in the center of such a photospheric line, will accurately "map-out" the stronger magnetic fields but with greater background noise than Z-photos, and with no polarity information.

## C. Causes of Weakenings

### 1. Zeeman Effects

One might first suppose that the weakening of a magnetically-sensitive Fraunhofer line in the presence of a strong magnetic field is due to the separation of the Zeeman components. To determine if this explanation can account for the observed weakening, we must know both the strength of the photospheric magnetic field and the shape of the intensity profile of the line at that point. Knowing the wavelength shift due to the field and the intensity

profile, $I(\lambda)$, the increase in the intensity at the line center, $\Delta I/I$, can be computed and compared with that seen by the spectroheliograph.

A method of determining $B_{\parallel}$, the line-of-sight magnetic field, with high spatial resolution is to obtain a Zeeman photograph (Z-photo). The details of obtaining a Z-photo have been described elsewhere (Leighton, 1959; Sheeley, 1964).

Figure 4(a) shows a Z-photo obtained during excellent seeing conditions. One can see many features of about 2000 km size which are not associated with sunspots and correspond to line-of-sight magnetic fields in the range 300-450 gauss. Even smaller features have fairly strong fields. On close examination of the original Z-photo, one can find magnetic fields with linear dimensions less than 800 km having line-of-sight field strengths of about 200-250 gauss. However, the fields of these tiny features are difficult to measure because of their small dimensions on the original Z-photo, consequently the actual field strength of these features may be higher than the measured value. Of those non-spot fields measured, none were found to have line-of-sight field strengths substantially greater

than about 500 gauss. Therefore, this value will be considered as a "typical" upper limit to $B_{\parallel}$ determined from Z-photos, regardless of the smallness of the feature.

Nevertheless, field strengths determined from Z-photos have several uncertainties. First, the calibration that has been used was derived from the mean photospheric line profile. There is some evidence from spectrograms of field regions that the slope of the line profile is less steep in field regions than in non-field regions, thus suggesting that if the profile from the field region were used for the calibration, the measured field strengths would be larger. Second, the absolute value of the fields measured on a Z-photo depends somewhat on the photographic reductions involved in cancelling the original plates (Sheeley, 1964). Third, since only $B_{\parallel}$ is measured by a "normal" Z-photo, the total field strength and its direction relative to the local vertical are not known even though these are the quantities desired. However, there is some preliminary evidence which suggests that photospheric non-spot fields do not deviate too far from the local vertical:

1. A transverse Z-photo, obtained on June 29, 1967, showed a strong transverse field in a sunspot penumbra but not associated with a neighboring plage, suggesting that if such fields were present, their strengths were probably less than a few hundred gauss. If these same features had typical line-of-sight fields of several hundred gauss, then the angle between the fields and the local vertical was probably less than 45°.

2. The measurement of the 70-100 gauss line-of-sight component of the field in a facula very near the limb of the sun ($\cos \theta = .07-.08$) indicated that if the field had a typical vertical strength of 200-500 gauss, then the field vector probably deviated no more than 10°-20° from the local vertical (Chapman and Sheeley, 1967).

3. Leighton (1959), from very limited data, found no evidence for strong transverse fields in faculae.

Now that we know approximately what to expect for the strength of the magnetic field in a weakening, it is necessary to know the shape of the intensity profile in order to determine the change in central intensity of a magnetically-sensitive line that would be expected from Zeeman splitting alone. The intensity profiles determined

from spectrograms were used in constructing Figure 7 which gives the predicted fractional intensity increase, $\Delta I/I$, at the line center versus the line-of-sight field strength for several simple Zeeman triplet lines often used for making spectroheliograms. For the typical measured upper limit to line-of-sight field strengths of 500 gauss, Figure 7 shows that $\Delta I/I$ is 0.09 for the $\lambda$6302.5 line and 0.10 for the $\lambda$5131.5 line. However, measured values of $\Delta I/I$, obtained from spectroheliograms in good seeing, run as high as about 0.45-0.50 for the $\lambda$6302.5 line and as high as about 0.55-0.60 for the $\lambda$5131.5 line. Although no magnetic field measurements are available for those spectroheliograms, if one adopts the typical upper limit of 500 gauss, then much of the weakening of these lines was due to non-Zeeman effects.

A similar conclusion is reached upon examining Figure 8 which shows $\Delta I/I$ for $\lambda$5131.5 versus $B_{\parallel}$ for the same features, the field being determined from the Ca I $\lambda$6103 Z-photo (Figure 4a) obtained an hour or so after the $\lambda$5131 spectroheliogram. Some of the scatter in Figure 8 may be partly due to the time difference between the two observations and partly to seeing. Again, the strength of the

Figure 7. Theoretical Values of $\Delta I/I$ Versus $B_{\parallel}$

These theoretical curves of $\Delta I/I$ versus $B_{\parallel}$ have been derived from field-free intensity profiles determined from spectrograms. The magnetic sensitivity for each line was used to convert wavelength from the line center into line-of-sight magnetic field strength, $B_{\parallel}$.

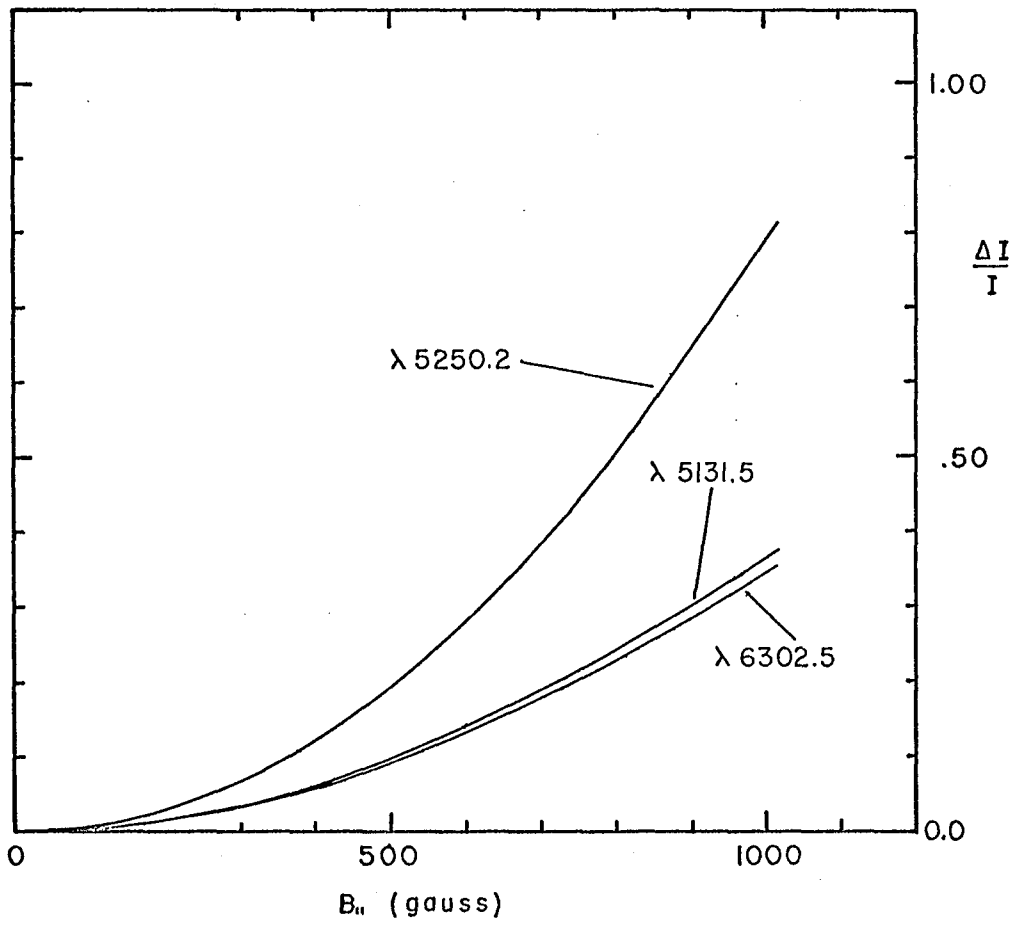


Fig. 7. Theoretical Values of $\Delta I/I$ Versus $B_{\parallel}$

Figure 8. Observed and Predicted $\Delta I/I$ from Z-photo and $\lambda 5131$ Spectroheliogram of August 13, 1967

The points show the observed $\Delta I/I$ for a number of features on the $\lambda 5131$ spectroheliogram of Figure 4(c) and the line-of-sight magnetic field strength for the same features from the Ca I $\lambda 6103$ Z-photo of Figure 4(a). All points lie a considerable distance above the curve predicted on the basis of Zeeman splitting alone, thus showing that Zeeman splitting cannot account for all of the observed weakening.

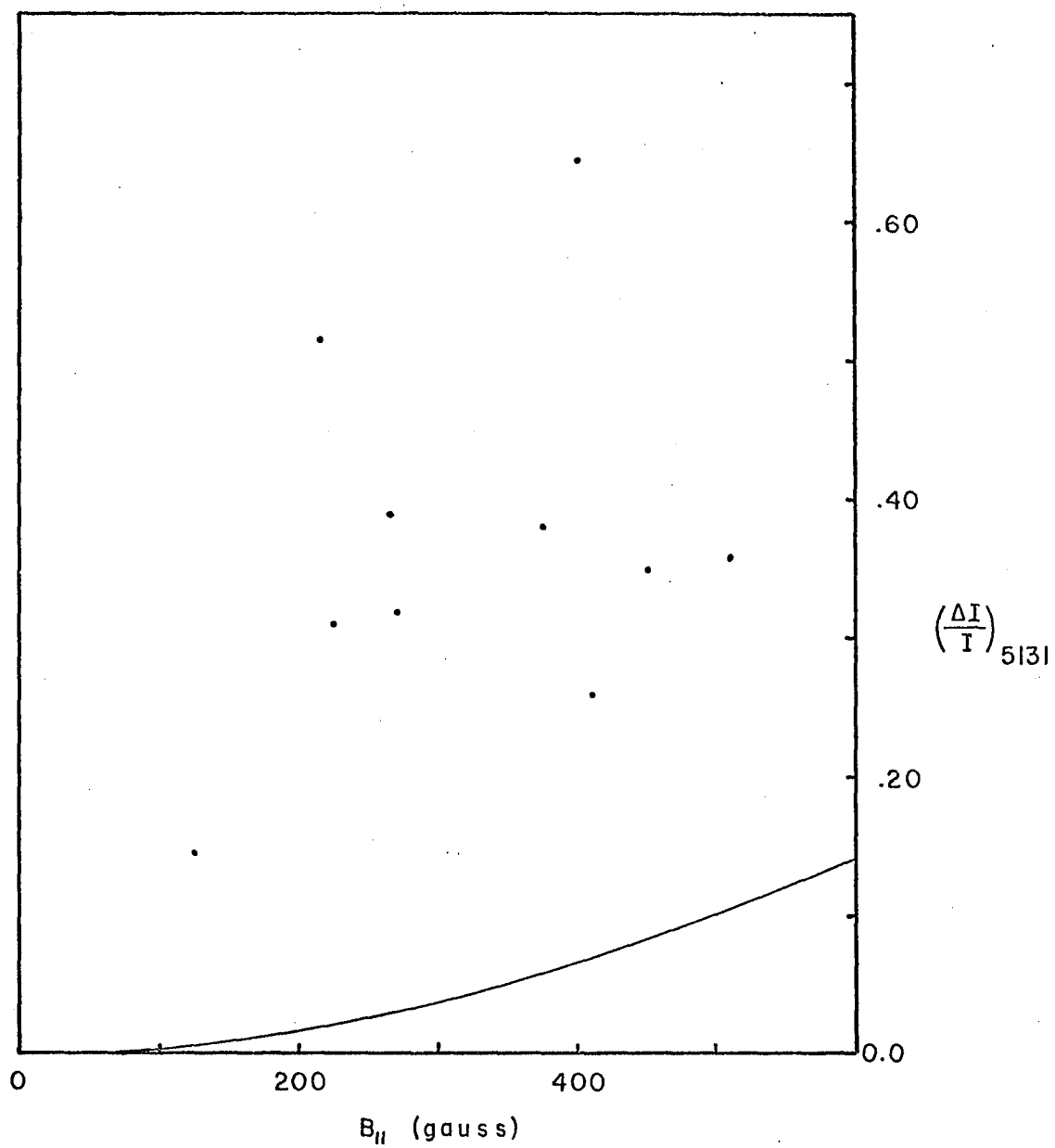


Fig. 8. Observed and Predicted $\Delta I/I$

magnetic field is not great enough to account for the observed $\Delta I/I$.

But what if the field were inclined to the line of sight and the total magnetic field, B , were therefore greater than $B_{\parallel}$? The predicted $\Delta I/I$ would also be greater. To determine the effect of field inclination, the following relation (for simple Zeeman triplets) is introduced,

$$\frac{\Delta I}{I} \approx \frac{1}{2} \frac{I''}{I} \left(\frac{\Delta\lambda}{B}\right)^2 B_{\parallel}^2 \left[1 + \frac{1}{2} \tan^2 \gamma\right]$$

where $I''$ is the second derivative of the intensity profile at the center of the line, $\frac{\Delta\lambda}{B}$ is the magnetic sensitivity, and $\gamma$ is the angle between the magnetic field direction and the line of sight. The expression, which makes use of a second-order Taylor series expansion for the line profile near its center, agrees approximately with the graphical relations in Figure 7 provided the Zeeman splitting due to the field is not too large (less than about 10 mA, corresponding to $\approx$340 gauss for the $\lambda$5131.5 line) such that the quadratic approximation to the line is not too bad. (For $\lambda$6302.5, $\frac{I''}{I} \approx 400$ $A^{-2}$, and for $\lambda$5250.2, $\frac{I''}{I} \approx 1800$ $A^{-2}$.) For $\gamma = 20°$, the predicted $\Delta I/I$ is increased only 7% over what would be predicted if the transverse field were zero, for example 10% becomes 10.7%, an amount not sufficient to

explain the amount of weakening observed on spectroheliograms solely on the basis of the Zeeman effect. For $\gamma = 45°$, the increase is 50%, for example 10% becomes 15%, still not enough to produce the measured $\Delta I/I$ of 55-60%.

Spectrographic Data: We have seen from spectroheliograms that the major part of the weakening of Fraunhofer lines is not due to Zeeman splitting. We will now show that data from spectrograms also supports this result. Weakenings on selected spectrograms will be studied to determine the relative importance of Zeeman and non-Zeeman effects. The amount of weakening expected directly from Zeeman splitting will be determined by computing the Zeeman shift due to the field and applying this to the intensity profile to find $(\Delta I/I)_Z$, the Zeeman part of the weakening. The magnetic field strength will be determined from the weakened spectrum line itself in the following way: If there were no other agency acting on the line except the magnetic field, then the absorption coefficient and the line would become broader in direct proportion to the strength of the field and the magnetic sensitivity of the line. If this were true, then the field strength would be given by $B = \frac{1}{2} \frac{\Delta FWHM}{(\Delta\lambda/B)}$, where $\Delta FWHM$ is the difference

between the full-width at half-maximum of the line in and out of field regions and $\Delta\lambda/B$ is the magnetic sensitivity. The direction of the field complicates the matter somewhat since the relative strength of the $\sigma$- and $\pi$- components depend on the direction of the field. Furthermore, there are non-Zeeman effects which will undoubtedly affect the width of the line in the field. However, if the fields are nearly line-of-sight as has been suggested previously, then we could determine $B_{\parallel}$ if we could allow for non-Zeeman width changes. By using two or more lines, having similar strength, from the same multiplet it should be possible to minimize the non-Zeeman effects for those lines. The field then would be given by the slope or rate-of-change of $\Delta$FWHM with increasing $\Delta\lambda/B$. Now there is no requirement that a line having zero magnetic sensitivity also have $\Delta$FWHM = 0; the magnetic field is now given by: $B = \frac{1}{2} \frac{\Delta(\Delta FWHM)}{\Delta(\Delta\lambda/B)}$ . Since most of the lines used from spectrograms are not simple Zeeman triplets, the determination of the Zeeman sensitivity will be explained.

For a simple Zeeman triplet the effective Zeeman sensitivity is just the separation per unit field strength, of one or the other of the $\sigma$-components from the center of

the line. The value of $\Delta\lambda/B$ is given by $\frac{\Delta\lambda}{B} = \frac{\mu_B}{hc} \lambda^2 \Delta(gM_J)$ where B is the total magnetic field strength and $\Delta(gM_J) = (g_2 M_{J2} - g_1 M_{J1})$ is the effective Landé g-factor. For more complicated Zeeman patterns there may be more than one $\sigma$-component (on each side of the center) and more than one $\pi$-component, in which case $\Delta(gM_J)$ is replaced by $\langle\Delta(gM_J)\rangle$ which is found by weighting each Zeeman component in the right (or left) half of the pattern by its relative intensity and then finding the weighted mean. The relative intensities were computed according to formulae given by White (1934). In some complicated Zeeman patterns, the $\pi$-components may shift away from the center of the line. Since the strength of the $\pi$-components relative to that of the $\sigma$-components is a function of the angle, $\gamma$, between the direction of the magnetic field and the line-of-sight, $\Delta\lambda/B$ is a function of $\gamma$. However, since preliminary evidence, mentioned previously, suggests that B may not deviate too far from line-of-sight, effective Zeeman sensitivities have been computed assuming $\gamma = 0$. Zeeman sensitivities computed assuming $\gamma = 0$ will be designated by $\Delta\lambda/B_{\parallel}$.

To illustrate how field strength is determined from changes in line width and the effect of field direction on

computed Zeeman sensitivities, some data will be presented for two weakenings and a small sunspot from a spectrogram in the λ6300 region obtained on October 26, 1967. Figure 9 shows ΔFWHM, from this data, versus $\Delta\lambda/B$ for three lines of 816 Fe I (multiplet number 816 of Fe I in the Revised Multiplet Table, Moore, 1945), one line of which (λ6302.5) is a simple Zeeman triplet. The cores of the three Zeeman components of λ6302.5 are resolved in the spot and their separation unambiguously gives a total field strength of 1450 gauss. Since the total field strength for this spot is known, it is instructive to check the known field strength against that determined from the splitting of the Zeeman components of the other two lines, whose effective Zeeman sensitivities depend on the field direction. Also, it will be interesting to compare the field that would be determined from ΔFWHM for the same lines with the known field thus gaining, perhaps, some idea of the reliability of the fields of weakenings determined from changes in FWHM.

As will be shown, the field in the sunspot seems to be highly inclined to the line-of-sight. The λ6301.5 and λ6336.9 lines are not simple Zeeman triplets therefore their effective Zeeman sensitivities depend on the

Figure 9. Magnetic Field Strengths from ΔFWHM Versus $\Delta\lambda/B$ for Spectrogram 2, October 26, 1967

The slopes of the lines give twice the magnetic field strength. The triangles represent ΔFWHM versus B in the sunspot. The open circles represent the separation of the resolved Zeeman components in the sunspot. The two lower pairs of circles connected by dashed lines show the extreme values in the computed $\Delta\lambda/B$ according to whether the field is along the line-of-sight (right-hand end of dashed line) or perpendicular to the line-of-sight (left-hand end of the dashed line). The uppermost open circle represents the resolved Zeeman components of the λ6302.5 line and gives a field strength of 1450 gauss in the spot.

The x and · symbols represent ΔFWHM versus $\Delta\lambda/B_{\parallel}$ in gaps 1 and 2, respectively. Although the slopes through all points indicate a B of 518 and 782 gauss, respectively, if only the end points are considered the fields are nearly the same and equal 690 gauss.

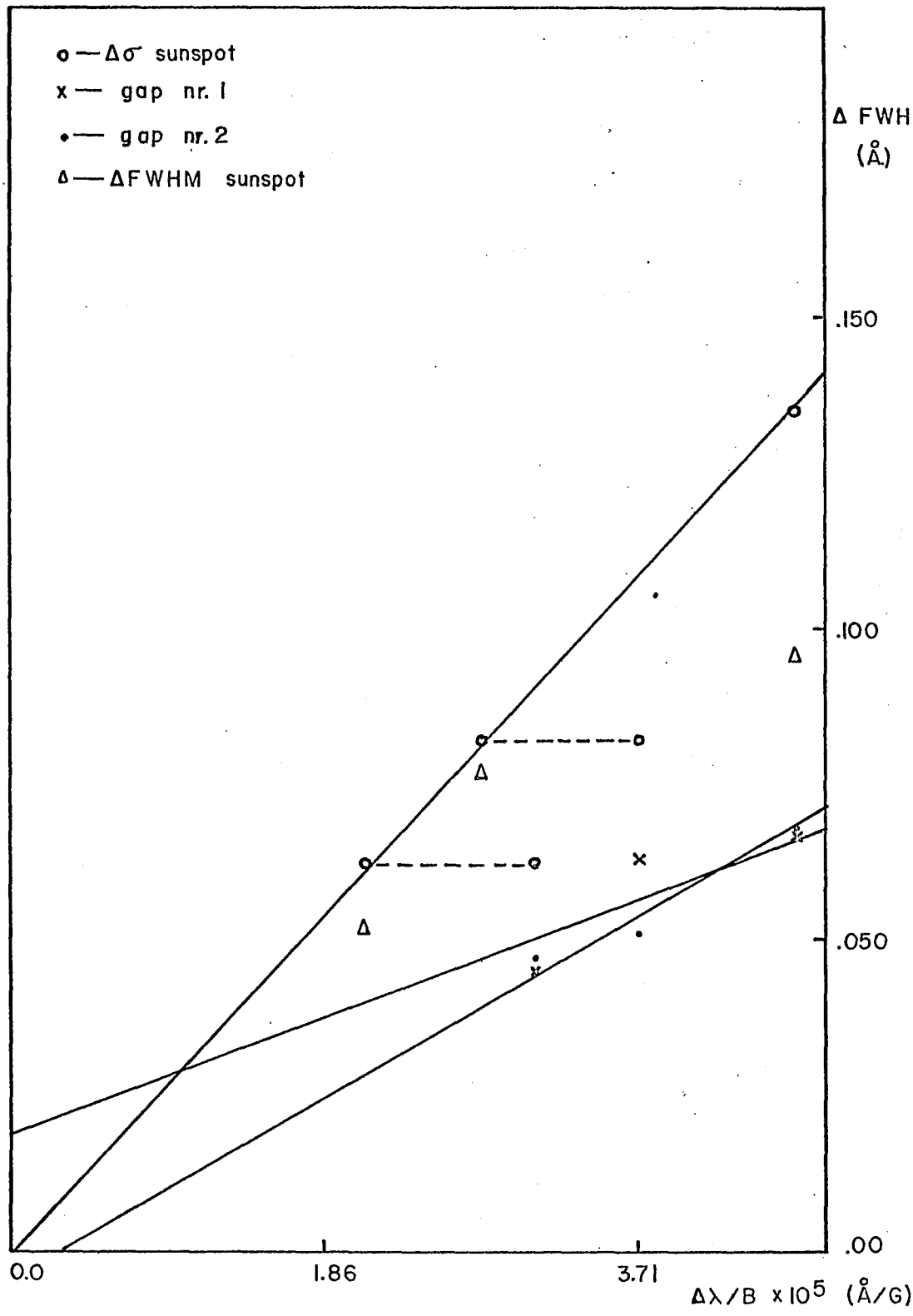


Fig. 9. Magnetic Field Strengths from ΔFWHM Vs. Δλ/B

direction of the magnetic field as has been discussed previously. For example, the effective Landé g-factor for λ6336.9 varies from 2.00 for a line-of-sight field to 1.50 for a completely transverse field. The two extremes in effective Zeeman sensitivity for λ6301.5 and λ6336.9 are shown connected by dotted lines in Figure 9. When the effective Zeeman sensitivities of these two lines are computed assuming a transverse field, they give very nearly the same B as the λ6302.5 line, but when their effective Zeeman sensitivities are computed assuming a line-of-sight field, these two spectrum lines give a rather different field than that given by the λ6302.5 line. Since all three lines give nearly the same B only when the effective Zeeman sensitivities of the two are computed for a completely transverse field, B may be almost completely transverse in the spot. The large inclination of the field seems to be confirmed by the presence of a strong $\pi$-component in the intensity profile of the λ6302.5 line. The weakness or absence of a scattered photospheric line in the intensity profile of the λ6336.9 line, whose $\pi$-components are shifted from the center of the line in the sunspot, suggests that scattered

light was not appreciable and hence not the cause of the strong $\pi$-component in $\lambda$6302.5.

If we now examine the plotted values of $\Delta$FWHM for these same lines in the spot, we find that, in Figure 9, two of the three, $\lambda$6301.5 and $\lambda$6336.9, define a line nearly parallel to and just below the 1450-gauss line determined from the resolved Zeeman components. The $\lambda$6302.5 line has too small a $\Delta$FWHM value, or conversely, the effective g-factor should be reduced from 2.5 to 1.9 in order to be in close agreement with the known field strength and $\Delta$FWHM for the other two lines. There is, therefore, more uncertainty to the field strength determined from $\Delta$FWHM than from the resolved Zeeman components of the lines. It is not too surprising then, that there is considerable uncertainty in the field strength determined from $\Delta$FWHM of the two weakenings (labeled gaps 1 and 2 in Figure 9). The field strengths determined are 518 $\pm$200-250 and 782 $\pm$100-150 gauss for gaps numbered 1 and 2, respectively. The indicated errors are estimates based on the scatter of $\Delta$FWHM above and below a straight line representing approximately the best fit to the observed $\Delta$FWHM points. The uncertainties in the slopes in Figure 9 are so large that it is

difficult to say whether the lines of this multiplet are wider or narrower in the gap than in the normal photosphere after allowing for the magnetic widening caused by the field.

Table 2 summarizes the measurements for the "gaps" shown in Figure 9. It is clear from this table that the inferred magnetic field strengths are of the same order of magnitude (at least no smaller than) as typically obtained from Z-photos, and that the corresponding Zeeman splittings are not enough to account for the measured $(\Delta I/I)$'s.

Data from several more spectrograms will be presented. As before, using the slope of $\Delta$FWHM versus $\Delta\lambda/B_{\parallel}$ for each gap or widening, in the manner previously described, $B_{\parallel}$ will be determined and then used, together with the shape of each line, to determine $(\Delta I/I)_Z$, the Zeeman part of the weakening. The non-Zeeman part of the weakening, $(\Delta I/I)_{NZ}$, will then be determined by subtracting $(\Delta I/I)_Z$ from the observed $\Delta I/I$.

Figure 10 shows $\Delta$ FWHM versus $\Delta\lambda/B_{\parallel}$ for lines of two multiplets, numbers 16 and 66, from a spectrogram (taken on October 26, 1967) that was not of outstanding quality. A particular advantage in using this wavelength

Table 2

Data for Three Lines of 816 Fe I from Spectrogram 2, October 26, 1967

Gap 1

| λ(A) | $\Delta(gM_J)$ | ΔI/I | $(\Delta I/I)_Z$ | $(\Delta I/I)_{NZ}$ |
|---|---|---|---|---|
| 6301.5 | 1.67 | 0.25 | 0.03 | 0.22 |
| 6302.5 | 2.50 | 0.46 | 0.17 | 0.29 |
| 6336.9 | 2.00 | 0.32 | 0.07 | 0.25 |

Gap 2

| λ(A) | $\Delta(gM_J)$ | ΔI/I | $(\Delta I/I)_Z$ | $(\Delta I/I)_{NZ}$ |
|---|---|---|---|---|
| 6301.5 | 1.67 | 0.26 | 0.08 | 0.18 |
| 6302.5 | 2.50 | 0.44 | 0.33 | 0.11 |
| 6336.9 | 2.00 | 0.33 | 0.15 | 0.18 |

Figure 10. Magnetic Field Strength for Spectrogram 1, October 26, 1967

The open circles represent values for 16 Fe I and the filled circles represent values for 66 Fe I. The line represents $B_{||}$ = 500 gauss and passes through the points representing λ5123.7 and λ5151.9, two nearly identical lines. The average slope for lines of both multiplets give the adopted field strength of 500 gauss.

Figure 11. Magnetic Field Strength for Spectrogram 16, September 10, 1966

The square represents the λ5129.2 line of 86 Ti II, the filled circle represents the λ5131.5 line of 66 Fe I, and the two open circles represent λ5123.7 and λ5127.4 of 16 Fe I. The slope of the line gives a field strength of 270 gauss. This field strength is probably too low, because the ΔFWHM for the λ5127.4 line (which is weaker than λ5123.7) gave a field strength in Figure 10 of 294 gauss whereas 500 gauss was more consistent with the nearly identically-shaped λ5151.9 line. Therefore, 500 gauss was adopted for this gap.

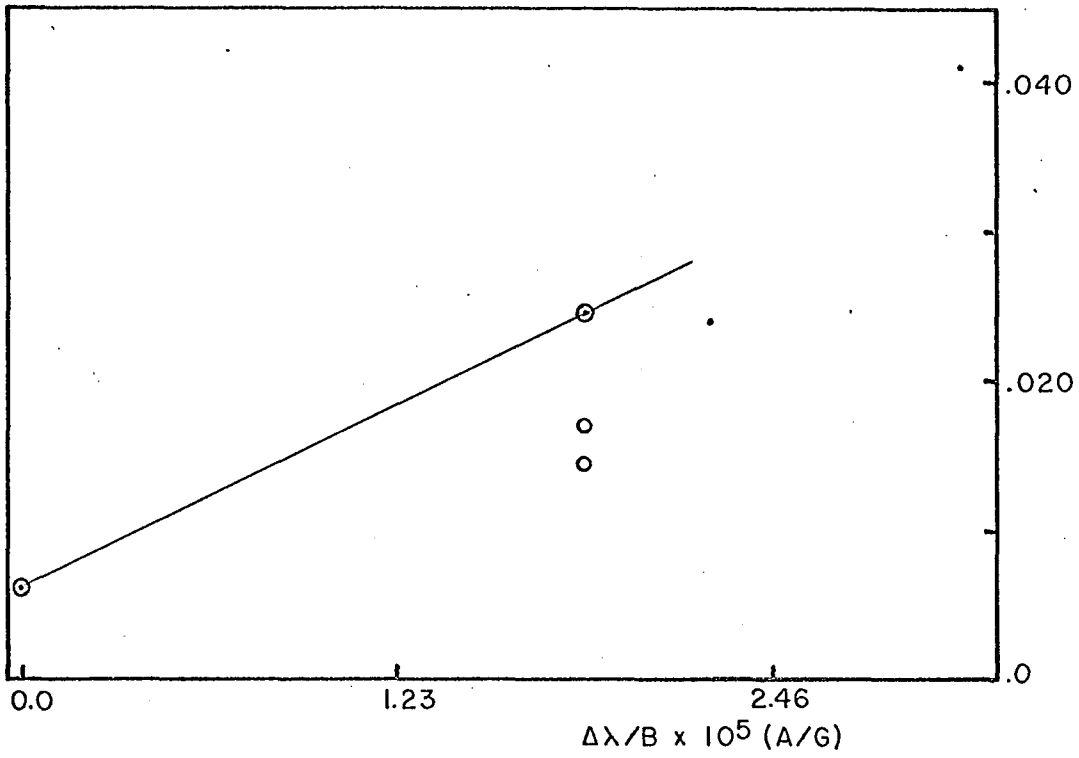


Fig. 10. Magnetic Field Strength for Spectrogram 1

Δ FWHM (A)

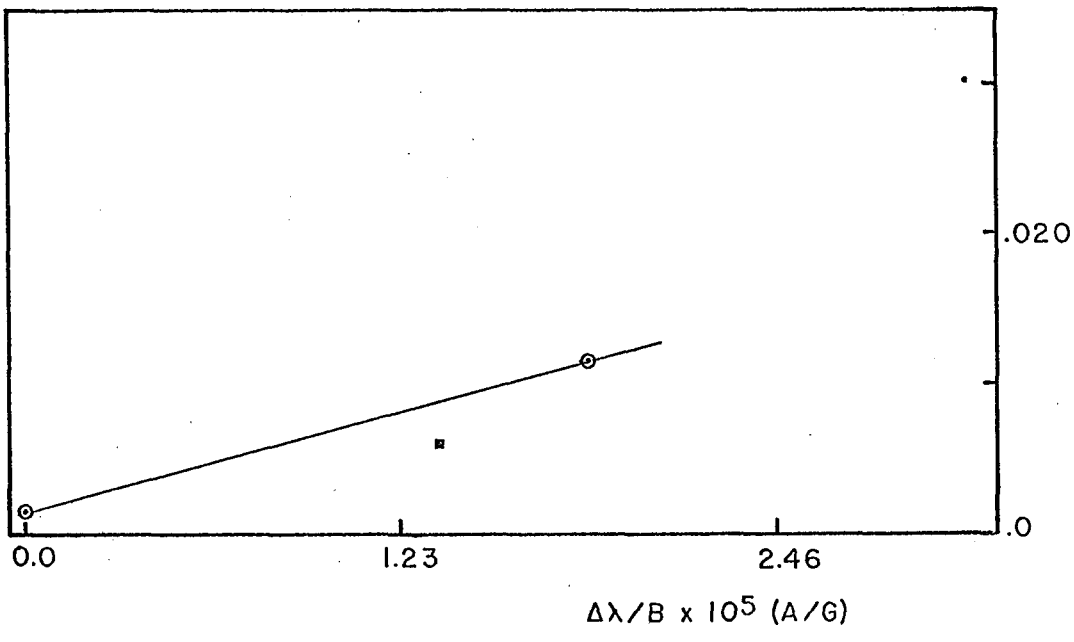


Fig. 11. Magnetic Field Strength for Spectrogram 16

region is the presence of the λ5123.7 line ($\Delta\lambda/B = 0$), several nearby similar strength lines of the same multiplet, as well as the simple Zeeman triplet line of high sensitivity, λ5131.5 of 66 Fe I. Figure 11 shows the same type of information for fewer lines in approximately the same wavelength region for a weakening from a spectrogram made during fairly good seeing by N. Sheeley on September 10, 1966. (Figure 12 shows the normal and weakened intensity profile of the λ5123.7 line from this spectrogram.) Table 3 gives the various determinations of $B_{\parallel}$ from the slopes in Figure 10. The indicated errors are based on the estimated accuracy in measuring ΔFWHM. Since these field strengths are for one feature, $B_{\parallel}$ is averaged to give 506 gauss. The field strength determined from the slope of ΔFWHM versus $\Delta\lambda/B$ for λ5123.7 and λ5127.4 in Figure 11 gives 270 gauss. However, by analogy with the fields determined from Figure 10 and Table 3, a field of 500 gauss is adopted rather than 270 gauss, since in Table 3, λ5123.7 and λ5127.4 gave only 294 gauss whereas the field adopted for that gap was 500 gauss. Table 4 and 5 give the observed values of $\Delta I/I$ for the spectrograms corresponding to Figure 10 and 11, respectively, as well as those values of $(\Delta I/I)_Z$ predicted on

Table 3 Determination of $B_{\parallel}$ from Spectrogram 1, October 26, 1967

| λ(A) | El. | $\Delta(gM_J)$ | $B_{\parallel}$ (gauss) |
|---|---|---|---|
| 5123.7 | 16 Fe I | 0.00 | |
| 5127.4 | 16 Fe I | 1.50 | 294 ±75 |
| 5131.5 | 66 Fe I | 2.50 | 1000 ±150 |
| 5145.1 | 66 Fe I | 1.83 | |
| 5150.8 | 16 Fe I | 1.50 | 230 ±50-75 |
| 5151.9 | 16 Fe I | 1.50 | 500 ±50-75 |

Table 4 Observed and Predicted $\Delta I/I$ for $B_{\parallel}$ = 500 gauss from Spectrogram 1, October 26, 1967

$(\Delta I/I)$ is the observed value, $(\Delta I/I)_Z$ is the value predicted from Zeeman splitting, and $(\Delta I/I)_{NZ}$ is the value arising from non-Zeeman effects.

| λ | EP(eV) | $(\Delta I/I)$ | $(\Delta I/I)_Z$ | $(\Delta I/I)_{NZ}$ |
|---|---|---|---|---|
| 5123.7 | 1.01 | 0.13 | 0.0 | 0.13 |
| 5127.4 | 0.91 | 0.23 | 0.04 | 0.19 |
| 5131.5 | 2.21 | 0.36 | 0.10 | 0.26 |
| 5145.1 | 2.19 | 0.26 | 0.04 | 0.22 |
| 5150.8 | 0.99 | 0.22 | 0.02 | 0.20 |
| 5151.9 | 1.01 | 0.24 | 0.02 | 0.22 |

Table 5

Data from Spectrogram 16, September 10, 1966

| λ(A) | El. | $\Delta gM_J$ | EP | $(\Delta I/I)_Z$ | $\Delta I/I$ | $(\Delta I/I)_{NZ}$ |
|---|---|---|---|---|---|---|
| 5123.7 | 16Fe I | 0.00 | 1.01 | 0.00 | 0.23 | 0.23 |
| 5127.4 | 16Fe I | 1.50 | 0.91 | 0.03 | 0.35 | 0.32 |
| 5129.2 | 86Ti II | 1.11 | 1.88 | 0.02 | 0.21 | 0.19 |
| 5131.5 | 66Fe I | 2.50 | 2.21 | 0.10 | 0.49 | 0.39 |

Table 6

Data from Spectrogram 2, September 27, 1967

| λ(A) | El. | $\Delta gM_J$ | EP | $(\Delta I/I)_Z$ | $\Delta I/I$ | $(\Delta I/I)_{NZ}$ |
|---|---|---|---|---|---|---|
| 6238.4 | 74Fe II | 1.47 | 3.87 | 0.04 | 0.11 | 0.07 |
| 6240.6 | 64Fe I | 1.00 | 2.21 | 0.04 | 0.20 | 0.16 |
| 6247.6 | 74Fe II | 1.10 | 3.87 | 0.05 | 0.11 | 0.06 |

Figure 12. Field and Field-Free λ5123.7 Profiles from Spectrogram 16, September 10, 1966

The intensity profiles of the magnetically-insensitive λ5123.7 line have been normalized to the same continuum intensity and superposed. The slight lateral shift is a result of the plotting procedure and has no physical significance.

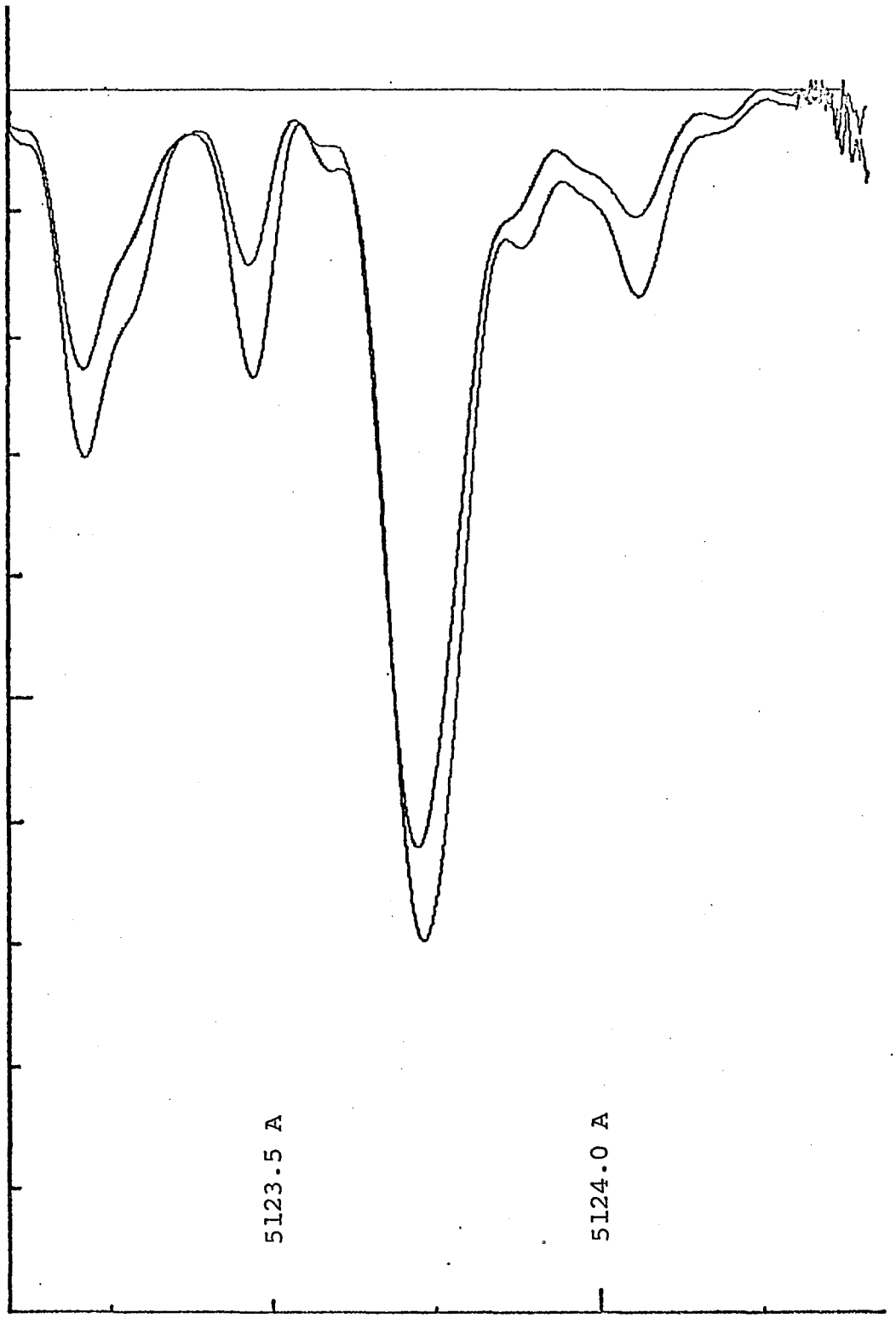


Fig. 12. Field and Field-Free Profiles

the basis of these inferred fields. In all cases, the non-Zeeman effect is larger than the predicted Zeeman effect in $\Delta I/I$.

One would expect that the Zeeman weakening of ionized lines would be a greater part of the observed weakening than in the case of neutral lines. Figure 13 shows $\Delta$FWHM versus $\Delta\lambda/B_{\parallel}$ for two lines of 74 Fe II and one line of 64 Fe I in the $\lambda$6200 region for a gap appearing on a fairly good spectrogram obtained on September 27, 1967. The slope of $\Delta$FWHM versus $\Delta\lambda/B_{\parallel}$ in Figure 13 gives a field strength of 810 gauss. Table 6 gives the Zeeman and non-Zeeman contributions to the observed $\Delta I/I$. The Zeeman contribution to $\Delta I/I$ is more nearly equal to the non-Zeeman contribution than for the neutral line $\lambda$6240.6. However, for Fe II the non-Zeeman contribution is still slightly greater than the Zeeman contribution. The negative intercepts on the ordinate axis hint at a slight non-Zeeman decrease in FWHM of the Fe II lines in the gap with perhaps a greater decrease indicated for the FWHM of the Fe I line, as might be expected because its $(\Delta I/I)_{NZ}$ is greater than for the Fe II lines.

Figure 13. Magnetic Field Strength for Spectrogram 2, September 27, 1967

The squares represent values for 74 Fe II and the filled circle represents values for λ6240.6 of 64 Fe I. The slope of the line indicates a magnetic field strength of 810 gauss.

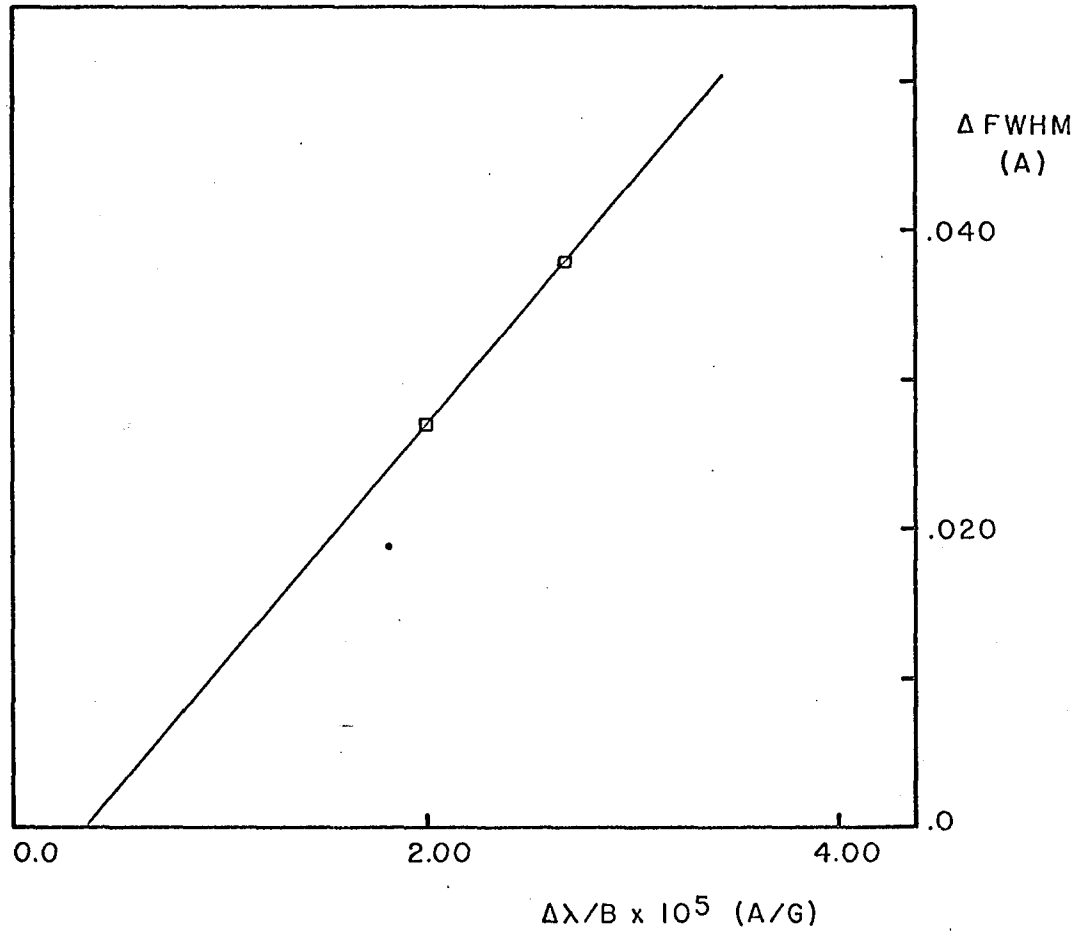


Fig. 13. Magnetic Field Strength for Spectrogram 2

Finally, data is presented for a wide variety of lines in the λ5250 region from a strong gap appearing on a spectrogram of outstanding quality taken by N. Sheeley on July 4, 1966. Table 7 gives the more important measured quantities for this spectrogram. (Figure 14 shows the gap and the gap-free intensity profiles for λ5250.2 of Fe I.) Figure 15 shows ΔFWHM versus $\Delta\lambda/B_{\parallel}$ for most of the lines on this spectrogram. The mean slope of ΔFWHM versus $\Delta\lambda/B_{\parallel}$ in Figure 15 for most lines indicates a magnetic field strength of about 400 gauss (but no higher than 500 gauss). Four lines on this spectrogram were remeasured with higher precision. The field strength of 500 gauss, determined from Figure 15, was then used to predict the amount of Zeeman weakening expected in these four lines based on a 500 gauss field and the shapes of their intensity profiles. This information is presented in Table 8. As one can see, the non-Zeeman contribution to the weakening of the λ5250.2 line is about 70% of the observed, total ΔI/I.

The λ5247.1 and λ5250.2 lines of 1 Fe I in the gap just discussed show that the use of ΔFWHM versus $\Delta\lambda/B_{\parallel}$ for lines of the same multiplet has its pitfalls. These two lines have very similar intensity profiles, yet the slope

Table 7

Data from Spectrogram 2, July 4, 1966

| λ(A) | El. | E.P. | W(mA) | $\Delta qM_I$ | ΔI/I | ΔFWHM | $\frac{\Delta W}{W}$ | ΔI | Spot |
|---|---|---|---|---|---|---|---|---|---|
| 5237.3 | 43Cr II | 4.07 | 49 | 1.33 | 0.10 | -- | -- | 0.05 | w |
| 5239.0 | 59Cr I | 2.71 | 16 | 1.50 | 0.08 | 0.003 | 0.27 | 0.06 | s |
| 5239.8 | 26Sc II | 1.45 | 55 | 1.00 | 0.18 | 0.005 | 0.12 | 0.09 | w |
| 5242.4 | 843Fe I | 3.63 | 80 | 1.00 | 0.42 | 0.009 | 0.10 | 0.12 | s |
| 5243.8 | 1089Fe I | 4.26 | 60 | 1.50 | 0.36 | 0.010 | 0.16 | 0.15 | s |
| 5246.8 | 23Cr II | 3.71 | 17 | 1.50 | 0.02 | 0.010 | 0.02 | 0.02 | w |
| 5247.1 | 1Fe I | 0.09 | 59 | 2.00 | 0.82 | 0.022 | 0.22 | 0.25 | S |
| 5247.6 | 18Cr I | 0.96 | 76 | 2.50 | 0.78 | 0.028 | 0.14 | 0.22 | s |
| 5249.1 | 1166Fe I | 4.47 | 30 | 0.92 | 0.11 | -0.002 | 0.23 | 0.07 | u |
| 5250.2 | 1Fe I | 0.12 | 62 | 3.00 | 0.94 | 0.023 | 0.27 | 0.28 | s |
| 5250.6 | 66Fe I | 2.20 | 104 | 1.50 | 0.45 | 0.011 | 0.11 | 0.12 | s |
| 5252.1 | 4Ti I | 0.05 | 16 | 1.50 | 0.13 | - | - | 0.10 | S |
| 5253.0 | 113Fe I | 2.28 | 16 | 1.00 | 0.09 | 0.002 | 0.28 | 0.07 | s |

Table 7, Continued

| λ(A) | El. | E.P. | W(mA) | $\Delta gM_J$ | ΔI/I | ΔFWHM | $-\frac{\Delta W}{W}$ | ΔI | Spot | |
|---|---|---|---|---|---|---|---|---|---|---|
| 5253.5 | 553Fe I | 3.27 | 75 | 1.50 | 0.51 | 0.014 | 0.14 | 0.16 | s | |
| 5255.0 | 1Fe I | 0.11 | 92 | 2.25 | 0.67 | 0.016 | 0.17 | 0.19 | s | blend |
| 5255.1 | 225Cr I | 3.46 | 38 | 1.30 | 0.19 | 0.012 | 0.19 | 0.12 | s | |
| 5255.3 | 32Mn I | 3.13 | 36 | 1.14 | 0.15 | 0.007 | 0.29 | 0.10 | s | |
| 5256.9 | 41Fe II | 2.89 | 18 | 1.66 | 0.06 | 0.012 | 0.14 | 0.05 | w | |
| 5257.6 | 188Co I | 3.97 | 20 | 1.21 | 0.09 | -0.009 | 0.38 | 0.07 | u | |
| 5260.4 | 22Ca I | 2.52 | 28 | 2.00 | 0.17 | 0.005 | 0.30 | 0.12 | s | |
| 5261.7 | 22Ca I | 2.52 | 99 | 1.25 | 0.46 | 0.010 | 0.12 | 0.13 | s | |
| 5262.2 | 22Ca I | 2.52 | 128 | 0.50 | 0.39 | - | - | 0.11 | s | |
| 5263.3 | 553Fe I | 3.26 | 121 | 1.50 | 0.41 | 0.017 | 0.04 | 0.10 | s | |
| 5263.9 | 788Fe I | 3.57 | 47 | 0.90 | 0.22 | -0.002 | 0.26 | 0.11 | u | |
| 5264.2 | 18Cr I | 0.97 | 101 | 2.00 | 0.52 | - | - | 0.13 | - | |
| 5264.8 | 48Fe II | 3.33 | 45 | 0.90 | 0.06 | 0.000 | 0.07 | 0.03 | w | |

Table 7, Continued

| λ(A) | El. | E.P. | W(mA) | $\Delta gM_J$ | ΔI/I | ΔFWHM | $-\frac{\Delta W}{W}$ | ΔI | Spot |
|---|---|---|---|---|---|---|---|---|---|
| 5265.6 | 22Ca I | 2.52 | 112 | 1.00 | 0.43 | 0.007 | 0.08 | 0.10 | s |
| 5265.7 | 18Cr I | 0.97 | 93 | 2.00 | 0.68 | - | - | 0.20 | S |
| 5266.0 | 156Ti I | 1.89 | 55 | 1.10 | 0.22 | 0.019? | 0.21? | 0.13 | s |
| 5266.6 | 383Fe I | 3.00 | 244 | 1.25 | 0.27 | -0.016 | 0.13 | 0.06 | s |
| 5269.5 | 15Fe I | 0.86 | 478 | 1.42 | 0.35 | -0.088 | 0.25 | 0.06 | S |

Figure 14. Field and Field-Free λ5250.2 Profiles from Spectrogram 2, July 4, 1966

The intensities have been normalized to the same continuum level. The equivalent width of λ5250.2 has decreased by 27% in the magnetic field region.

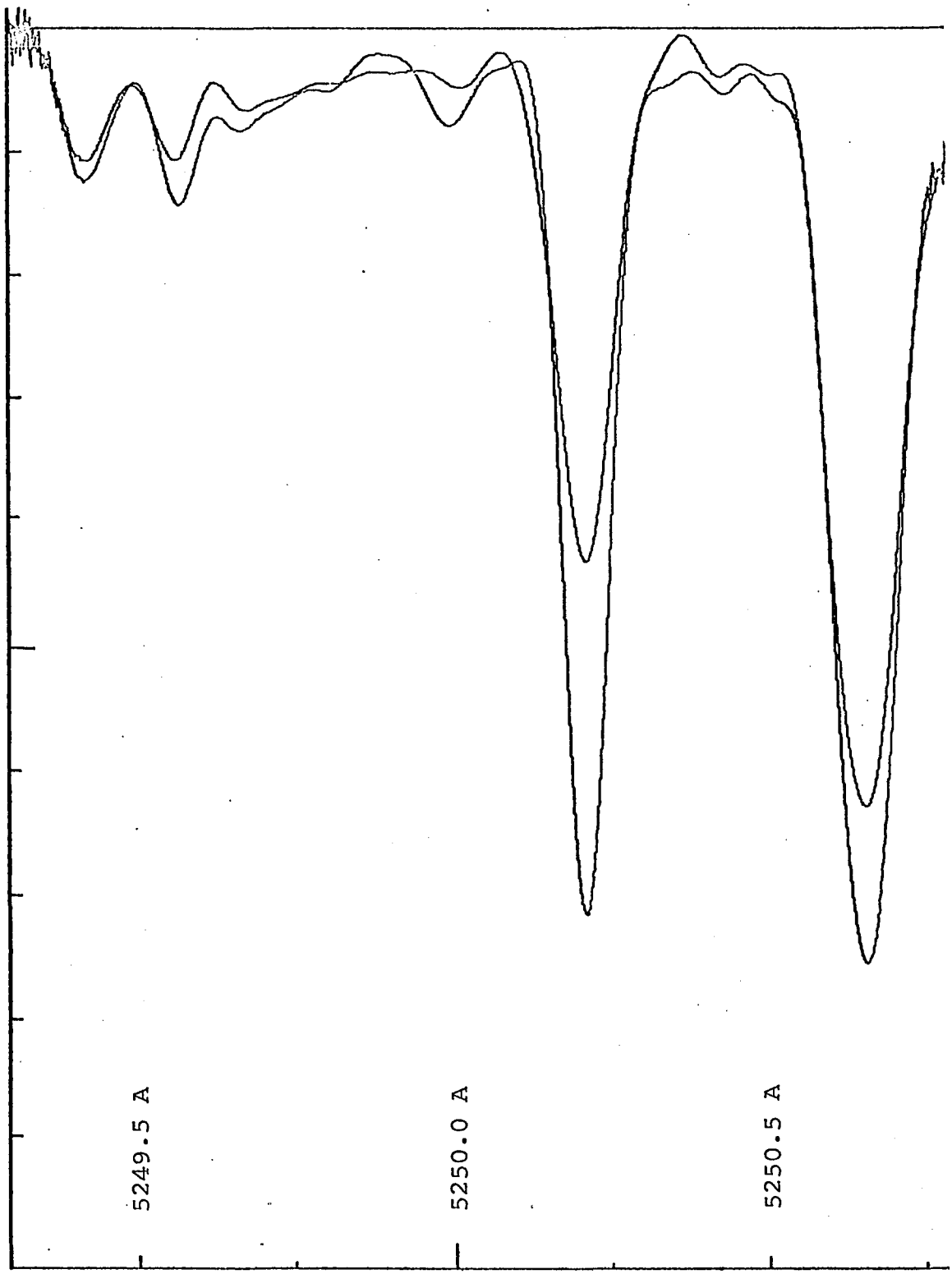


Fig. 14. Field and Field-Free Profiles

Figure 15. Magnetic Field Strength for Spectrogram 2, July 4, 1966

The lower solid line has a slope corresponding to a magnetic field strength of 400 gauss. It is quite possible that the field could be 500 gauss (upper solid line) which is the field strength used in Table 8. Most of the points near the bottom of the figure correspond to ions or lines that are much weaker than λ5250.2-type lines. The dotted line connects the λ5247.1 and λ5250.2 lines and indicates a magnetic field strength of 38 gauss, quite inconsistent with the field strength determined from the other lines.

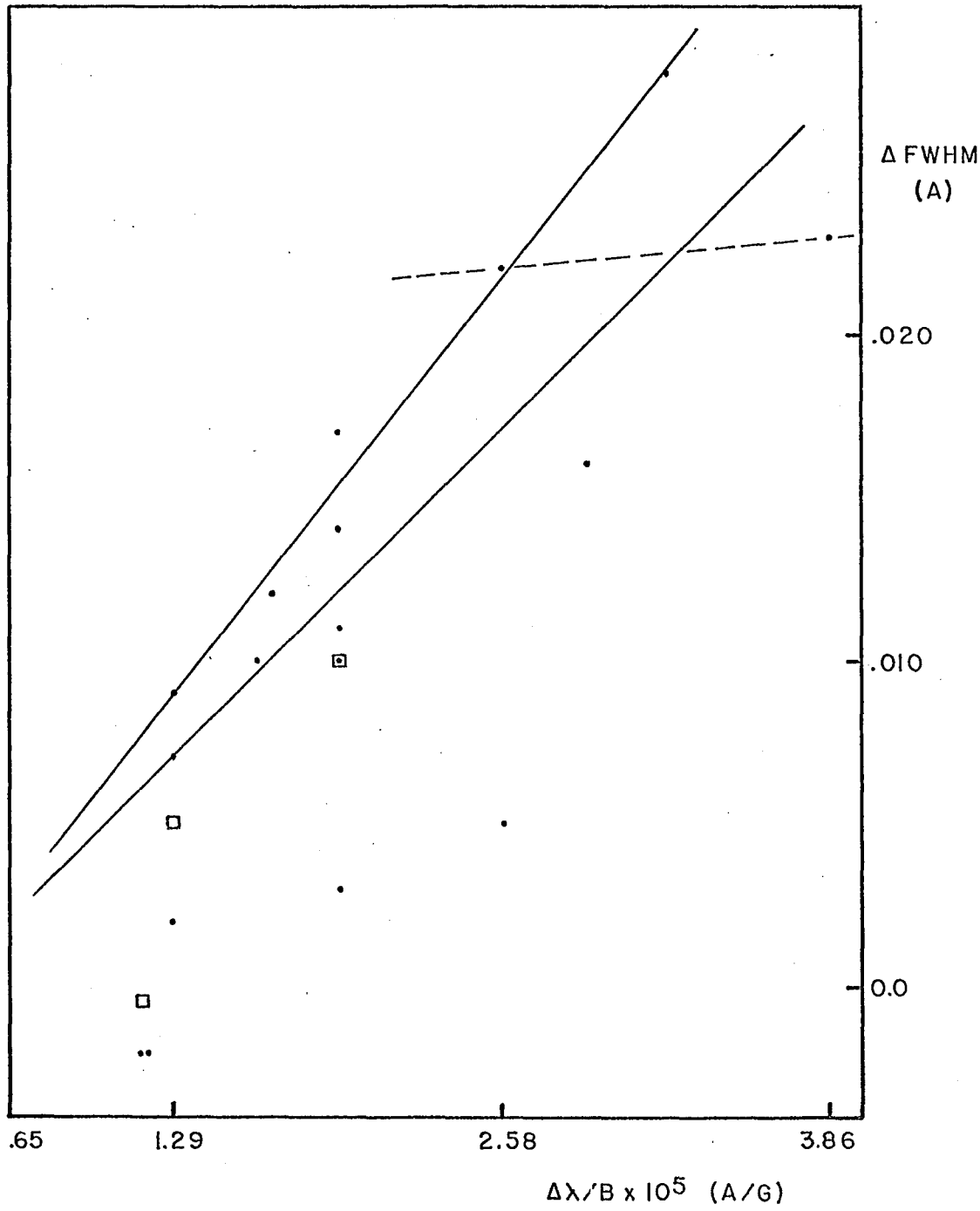


Fig. 15. Magnetic Field Strength for Spectrogram 2

Table 8

Higher Accuracy Data from Spectrogram 2,

July 4, 1966

| λ(A) | El. | $\Delta gM_J$ | EP | $(\Delta I/I)_Z$ | $\Delta I/I$ | $(\Delta I/I)_{NZ}$ |
|---|---|---|---|---|---|---|
| 5247.1 | 1Fe I | 2.00 | 0.09 | 0.16 | 0.96 | 0.80 |
| 5247.6 | 18Cr I | 2.50 | 0.96 | 0.16 | 0.87 | 0.71 |
| 5250.2 | 1Fe I | 3.00 | 0.12 | 0.30 | 1.02 | 0.72 |
| 5250.6 | 66Fe I | 1.50 | 2.20 | 0.05 | 0.57 | 0.52 |

of ΔFWHM versus $\Delta\lambda/B_{\parallel}$ in Figure 15 (dotted line) indicates a field strength of 38 gauss whereas 400 gauss is more consistent with the other data. The reason for the discrepancy may lie with the λ5250.2 line since the λ5247.1 line seems to have a value of ΔFWHM that is consistent with much of the other data, but λ5250.2 seems to have too small a value for ΔFWHM to be consistent with the other data. A possible explanation might be that the saturation of the 5250 line has been largely removed by magnetic splitting whereupon the non-Zeeman effects become relatively more important than for the 5247 line.

In summary, for field strengths determined from both Z-photos and spectrograms, the direct effect of Zeeman splitting can account for only a fraction, often much less than one-half, of the observed weakening. To explain most or all of the observed weakening by Zeeman splitting would require magnetic fields of well over 1000 gauss for which there is no evidence in this investigation.

2. Non-Zeeman Effects

a. Direct evidence. Direct evidence for non-Zeeman effects comes from spectroheliograms made in magnetically-insensitive lines ($\Delta\lambda/B = 0$). Such

spectroheliograms show weakenings in the same places that Z-photos show magnetic fields [see Figure 3(a) and (d)]. Tables 9 and 10 give some typical values of $\Delta I/I$ from spectroheliograms made in Zeeman-insensitive lines. The weakening of Zeeman-insensitive lines in magnetic field regions shows that the physical conditions of the solar atmosphere are modified by the presence of the relatively strong (B >200 gauss) magnetic fields. One of the most dramatic consequences of this change is the well-known appearance of chromospheric emission in the H and K lines of Ca II. Spectrograms of the $\lambda$5123.7 line showed weakenings which gave values of $\Delta I/I$ consistent with the range of values found from spectroheliograms. Weakenings also appeared on a spectrogram of $\lambda$5434 which, however, was too heavily exposed to measure. The determination of the background intensity becomes more difficult for strong lines such as $\lambda$5434. On spectroheliograms in $\lambda$5434.5 and, to a lesser degree, in $\lambda$5123.7, the field-free photosphere is rather complicated. Many locally-bright areas are seen which do not correspond to places where strong photospheric magnetic fields are found.

Table 9

Average ΔI/I for Various Features

from Spectroheliograms, June 28, 1967

| El. λ(A) | 687 Fe I 4863 | 15 Fe I 5434 |
|---|---|---|
| Mean ΔI/I for Various Features | 0.09 | 0.16 |

Table 10

Measured ΔI/I of Magnetically-Insensitive Lines

for the Same Features from Spectroheliograms

of August 28, 1967

| El. λ(A) / Feature | 1087 Fe I 5691.5 | 16 Fe I 5123.7 | 686 Fe I 5576.1 | 15 Fe I 5434.5 |
|---|---|---|---|---|
| 1 | 0.10 | 0.14 | 0.14 | 0.21 |
| 2 | - | 0.14 | 0.17 | 0.26 |
| 3 | 0.07 | 0.16 | 0.16 | 0.24 |
| 4 | 0.08 | 0.20 | 0.22 | 0.34 |
| 5 | 0.10 | 0.15 | 0.11 | 0.25 |

Simultaneous spectroheliograms have been obtained in several pairs of lines, each pair having one line which is magnetically sensitive and the other magnetically insensitive. Figures 16, 17, and 18 show the measured values of $\Delta I/I$ for a number of more easily identified features that were well defined on each spectroheliogram of the pair. The features on the three pairs of spectroheliograms are unrelated to each other. Only $\lambda 5131$ is a simple Zeeman triplet. For each pair, the Zeeman-sensitive line has the greater amount of weakening, on the average, than the Zeeman-insensitive line. However, the weakening of the Zeeman-insensitive line is not much less than that of the Zeeman-sensitive line, suggesting that the non-Zeeman effects dominate the Zeeman effects for these lines.

b. Effects of Ionization State. One might consider that a possible explanation for the non-Zeeman weakening of Fraunhofer lines is that the temperature is higher in a non-spot magnetic field and therefore the atoms will tend to be in higher states of excitation and ionization than in surrounding field-free regions. If this were true, then the lines belonging to ions should tend not to weaken as much as lines of neutral atoms. Similarily, lines that

Figure 16. Measured Values of $\Delta I/I$ from Simultaneous Spectroheliograms in $\lambda 4855$ and $\lambda 4863$

The straight line in the figure is at a 45° angle and indicates a hypothetical 1:1 relation between the two axes. One can see that the values of $\Delta I/I$ for the magnetically-sensitive line $\lambda 4855$ tend usually to be only slightly greater than those for the magnetically-insensitive $\lambda 4863$ line, showing that Zeeman splitting is a relatively unimportant contributor to $\Delta I/I$ for these lines.

Figure 17. Measured Values of $\Delta I/I$ from Simultaneous Spectroheliograms in $\lambda 5131$ and $\lambda 5124$

The straight line indicates a hypothetical 1:1 relation between the two axes. Although the Zeeman effect contributes to $\Delta I/I$ for $\lambda 5131$, it would seem that the non-Zeeman part is dominant since many of the points are not far above the 1:1 line.

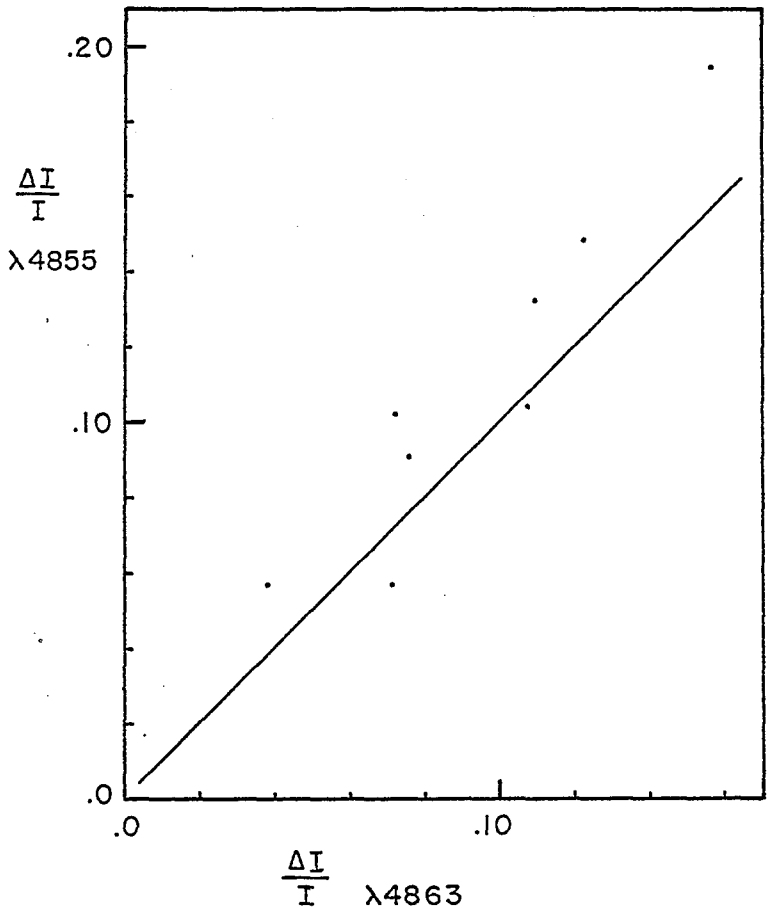


Fig. 16. Measured Values of ΔI/I

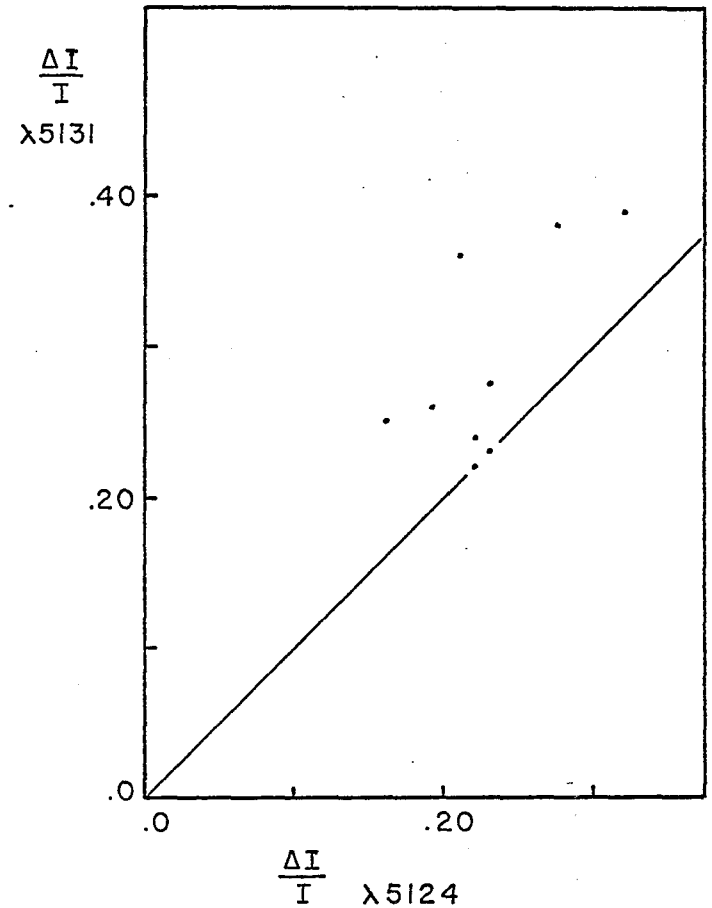


Fig. 17. Measured Values of ΔI/I

Figure 18. Measured Values of $\Delta I/I$ from Simultaneous Spectroheliograms in $\lambda 5410$ and $\lambda 5434$

Although there is much scatter it seems that the magnetically-sensitive $\lambda 5410$ line is usually weakened more than the magnetically-insensitive $\lambda 5434$ line. However, non-Zeeman effects again seem to be the major contributor to $\Delta I/I$.

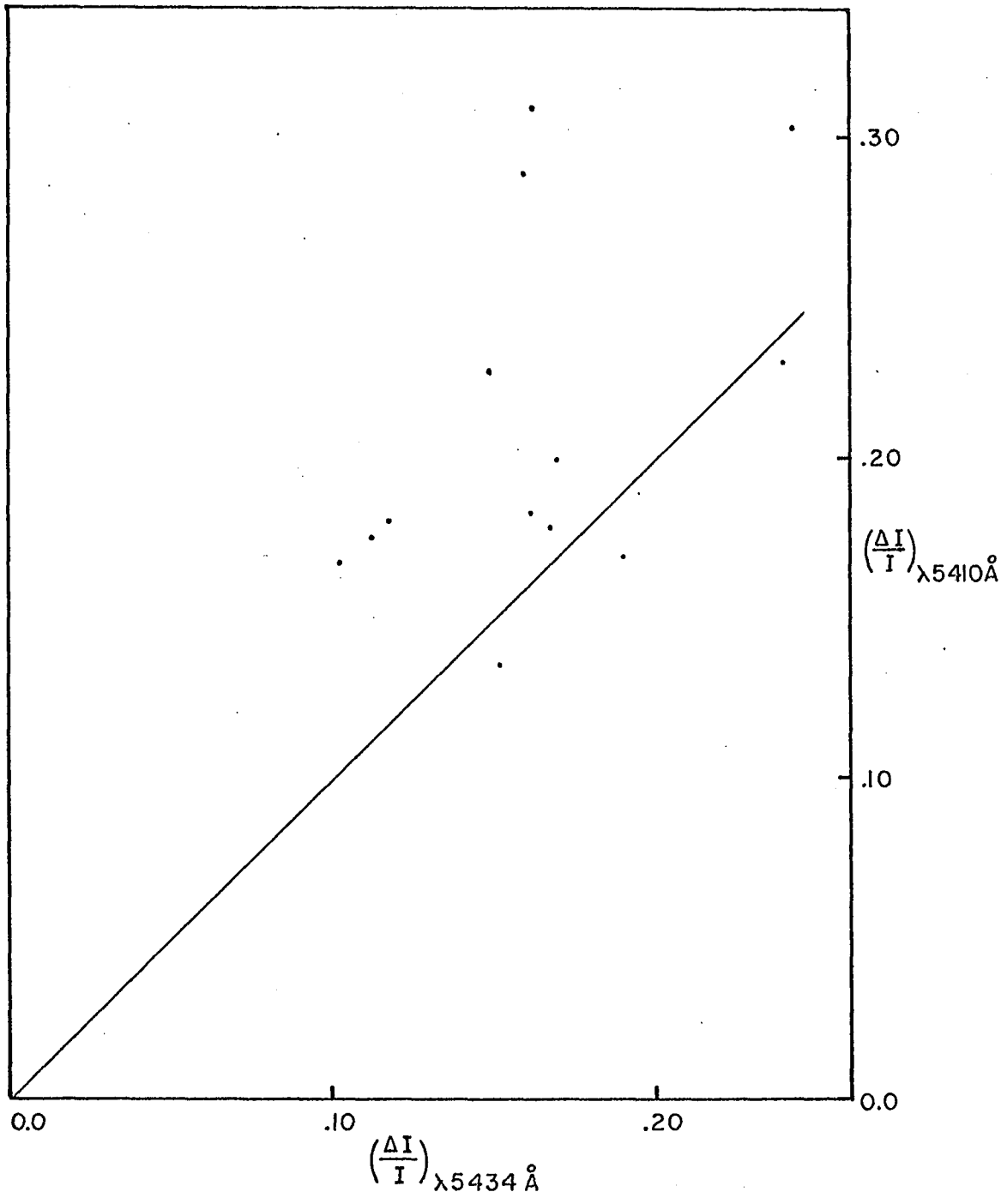


Fig. 18. Measured Values of $\Delta I/I$

weaken in sunspots, which are cool regions, might tend to, if not strengthen, weaken less in non-spot field regions than lines that strengthen in sunspots. To test this rough hypothesis, lines of ions and lines with a W-designation (indicating that the line appears to weaken appreciably in sunspots) in the Second Revised Rowland Table (NBS Monograph 61, 1966) were chosen which were suitable for making spectroheliograms. Almost without exception spectroheliograms in these lines show no obvious sign of the usual weakenings associated with magnetic fields. Figure 19 shows two pairs of spectroheliograms, each pair made simultaneously. One line of each pair is a Fe II line and the other a Fe I line. The differences between λ6240.6 of Fe I and λ6247.6 of 74 Fe II are easy to see while the differences between λ5250.2 of 1 Fe I and λ5264.8 of Fe I are striking. Table 11 presents measurements of the weakening on the λ6240.6 Fe I and λ6247.6 Fe II spectroheliograms. Since nearly all of the features appearing on the λ6240.6 Fe I spectroheliogram could not even be seen on the λ6247.6 Fe II spectroheliogram, $\Delta I/I$ values given for the latter are upper limits.

Figure 19. Simultaneous Spectroheliograms in Lines of Neutral and Ionized Atoms

Pair Above: The high contrast in λ5250.2 is very striking, especially when compared to the absence of bright features on the simultaneous λ5264.8 spectroheliogram. Although the Fe II line is somewhat weaker than the Fe I line, we must conclude that photospheric lines of ions do not show locally-bright regions on spectroheliograms and are therefore not appreciably weakened in field regions.

Pair Below: These two lines have very similar strengths and Zeeman sensitivities. The λ6247.6 spectroheliogram has lower contrast than the λ6240.6 spectroheliogram showing again, that photospheric lines of ions are not appreciably weakened in magnetic field regions.


PAIR ABOVE: FEBRUARY 5, 1968

17,000 KM

PAIR BELOW: SEPTEMBER 30, 1967

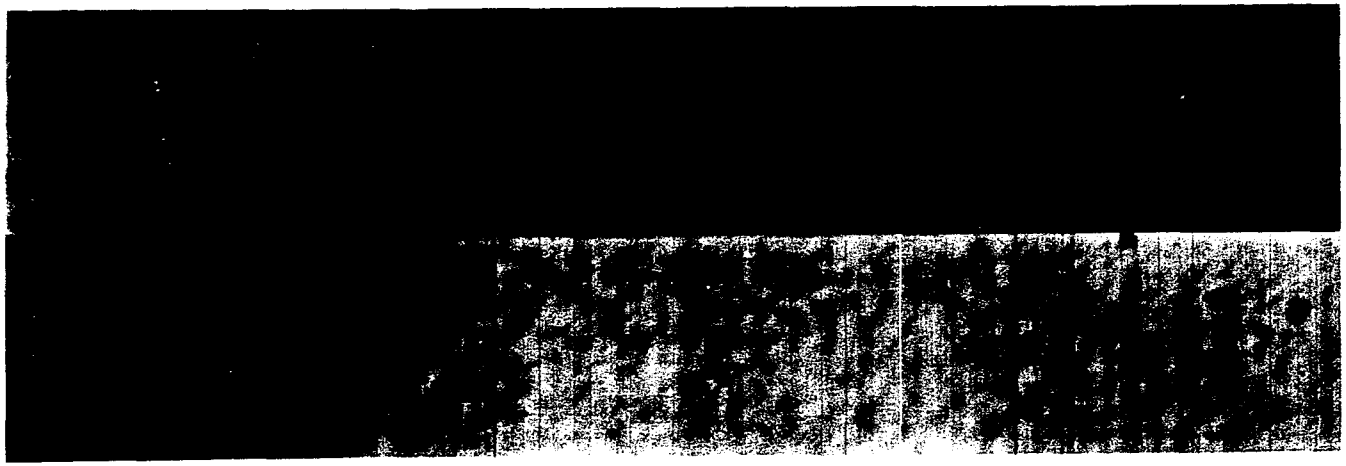


Fig. 19

Table 11

Weakening of λ6240.6 of Fe I and λ6247.6 of Fe II

Determined from Spectroheliograms

| Feature | Fe I ΔI/I | Fe II ΔI/I |
|---|---|---|
| 1 | 0.06 | 0.04 |
| 2 | 0.07 | 0.06 |
| 3 | 0.14 | 0.04 |
| 4 | 0.14 | 0.06 |
| 5 | 0.06 | 0.04 |

Table 12

Weakening of Lines of Ions

for Unrelated Gaps from Spectrograms

| λ | El. | W | E.P. | ΔW | ΔI/I | $\Delta I/I_c$ |
|---|---|---|---|---|---|---|
| 6238.4 | 74Fe II | 41 | 3.87 | -0.3 | 0.11 | 0.08 |
| 6247.6 | 74Fe II | 49 | 3.87 | +0.6 | 0.11 | 0.07 |
| 6416.9 | 74Fe II | 48 | 3.89 | +0.4 | 0.14 | 0.09 |
| 6432.7 | 40Fe II | 38 | 2.89 | +2.4 | 0.15 | 0.10 |
| 5239.8 | 26Sc II | 55 | 1.45 | -5.6 | 0.18 | 0.09 |
| 5246.8 | 23Cr II | 17 | 3.71 | -0.3 | 0.02 | 0.02 |
| 5264.8 | 48Fe II | 45 | 3.33 | -3.1 | 0.06 | 0.03 |
| 5129.2 | 86Ti II | 70 | 1.88 | -3.- | 0.21 | 0.11 |

Spectrograms have shown that lines of ions are weakened, but not by an appreciable amount. Table 12 gives $\Delta I/I_c$ and $\Delta W$, the fractional change of the central intensity in units of the continuum and the change in the equivalent width in mA, for lines of ions from spectrograms of unrelated weakenings. The changes in central intensity and equivalent width are quite small and for some lines the measured values are smaller than the uncertainties of measurement.

Near its core, the very strong K-lines of the Ca II ion has strong emission corresponding approximately to photospheric magnetic field regions. The contrast between field and non-field regions is greater in the core than elsewhere in the line, a situation which is the reverse of that for the neutral Ca I line at $\lambda$4227 (Figure 3). For these two lines, whose cores are formed in the chromosphere, the effect in the field regions is greater for the ion than for the neutral line, whereas in the photosphere, the reverse was the case, i.e. lines of neutral atoms had more contrast than lines of ions in and out of magnetic field regions.

c. Effects of Height-of-Formation. Since the density, pressure and temperature of the solar atmosphere vary with height, one might expect that the weakening of lines due to the non-Zeeman effect in field regions, would also depend on height. Some evidence, shown in Figures 20 and 21, indicates that there is little, if any, dependence on height for the lines shown there. Each point corresponds to the average of a number of weakenings on that spectroheliogram. The upper points in each figure are observed values of $\Delta I/I$, whereas the lower values are $\Delta I$ in units of the continuum derived from the observed values by multiplying the former by their respective central intensities (taken from the Utrecht solar atlas). Since these lines are magnetically insensitive, the Zeeman effect does not affect the results. The equivalent width of the line has been used as an indication of the line's height of formation. Over the range of equivalent widths encompassed by these lines, the change of intensity in fractions of the continuum intensity, does not show any noticeable dependence on equivalent width.

Another way of looking at different heights in the solar atmosphere is to view the sun in different parts of a

Figure 20. $\Delta I/I$ and $\Delta I$ from Spectroheliograms in Magnetically-Insensitive Lines Versus Equivalent Width, June 1967

The open circles represent the mean $\Delta I/I$ for a number of features measured on spectroheliograms taken in magnetically-insensitive lines on June 28, 1967. The dots represent $\Delta I$, in units of the continuum intensity, obtained by multiplying the observed $\Delta I/I$ by the central intensity of the line determined from the Utrecht atlas. There seems to be no strong dependence of $\Delta I$ on W.

Figure 21. $\Delta I/I$ and $\Delta I$ from Spectroheliograms in Magnetically-Insensitive Lines Versus Equivalent Width, August 1967

The open circles represent the mean $\Delta I/I$ for a number of features measured on spectroheliograms taken in magnetically-insensitive lines on August 28, 1967. The dots represent $\Delta I$, in units of the continuum intensity, obtained by multiplying the observed $\Delta I/I$ by the central intensity of the line determined from the Utrecht atlas. The x represents the $\lambda 5691.5$ line which may be partly blended. Again, there seems to be no strong dependence of $\Delta I$ on W, the equivalent width.

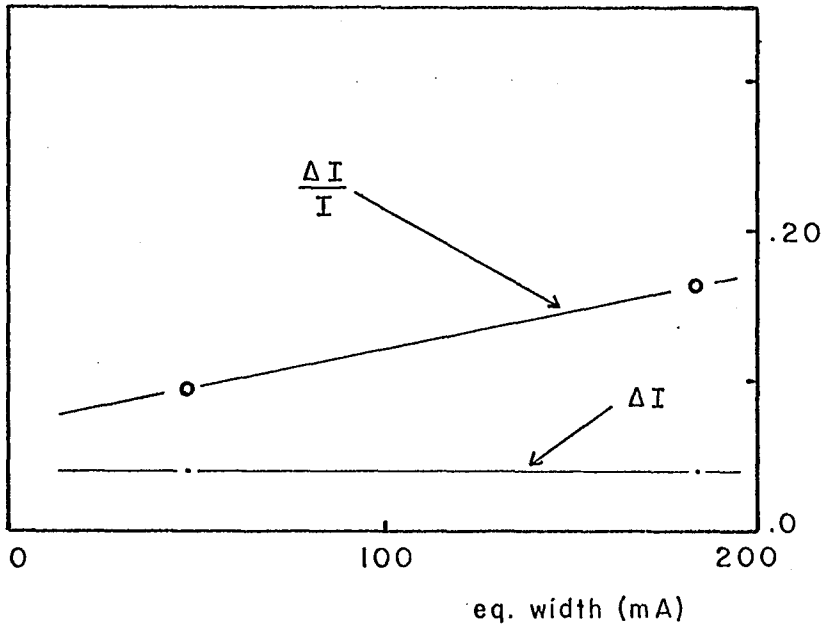


Fig. 20. ΔI/I and ΔI from Spectroheliograms

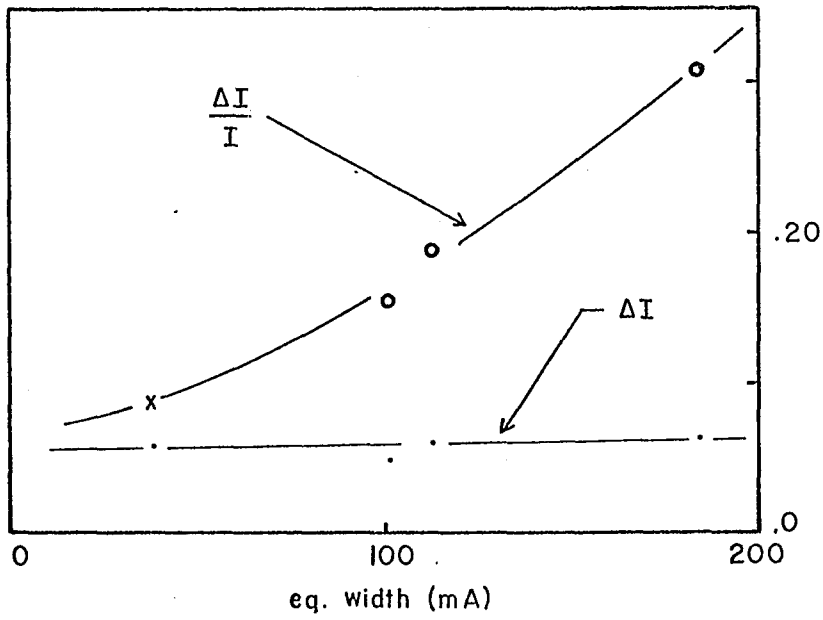


Fig. 21. ΔI/I and ΔI from Spectroheliograms

spectrum line. In the core of a line, where the line absorption coefficient is greatest, one is looking higher in the atmosphere than in the wings of the line. The $\Delta I/I$ was measured for a number of features appearing on the $\lambda$4227 spectroheliogram of Figure 3 in the core and the violet wing (.20A from the line center). Table 13 gives the mean of the measured values of $\Delta I/I$, the mean values of $\Delta I$ normalized to the same background intensity, and mean values of $\Delta I$ in fractions of the continuum intensity, using the intensity profile from the Utrecht atlas. There is much more contrast on the spectroheliograms taken in the wing than on the one taken in the core. Since this line is so broad, Zeeman shifts and Doppler shifts should not be important at these two wavelengths. Therefore, since $\Delta I/I_c$ is much greater in the wings than in the core, the effect of the altered physical conditions in the field regions is greater, lower (where the wings are formed) than higher (where the core is formed). Figures 22 and 23 show $\Delta W/W$ and $\Delta I/I_c$, respectively, versus their equivalent width for most lines of Table 7 (Spectrogram 2, July 4, 1966, $\lambda$5250 region). The effect of Zeeman splitting has not been removed from this data; however, in section 1 it was

Table 13

Measured Values of $\Delta I/I$

for Ca I $\lambda 4227$

| Feature | Core | Wing |
|---|---|---|
| 1 | 0.16 | 0.19 |
| 2 | 0.12 | 0.20 |
| 3 | 0.12 | 0.14 |
| 4 | 0.16 | 0.21 |
| 5 | 0.09 | 0.12 |
| Mean $\Delta I/I$ | 0.13 | 0.17 |
| Mean $\Delta I/I$ Relative to Same Background Intensity | 0.22 | 0.79 |
| Mean $\Delta I$ in Fractions of Continuum Intensity | 0.03 | 0.14 |

Figure 22. Fractional Changes in Equivalent Width versus Equivalent Width, Spectrogram 2, July 4, 1966

Stronger lines, which probably tend to be formed higher than weaker lines, generally have smaller percentage decreases in their equivalent widths. The lines of ions are represented by squares.

Figure 23. Fractional Changes in Central Intensity versus Equivalent Width, Spectrogram 2, July 4, 1966

The change in central intensity, in units of the continuum intensity, is similar for strong and weak lines but seem to be slightly larger for lines between 60-100 mA in equivalent width. The lines of ions are represented by squares.

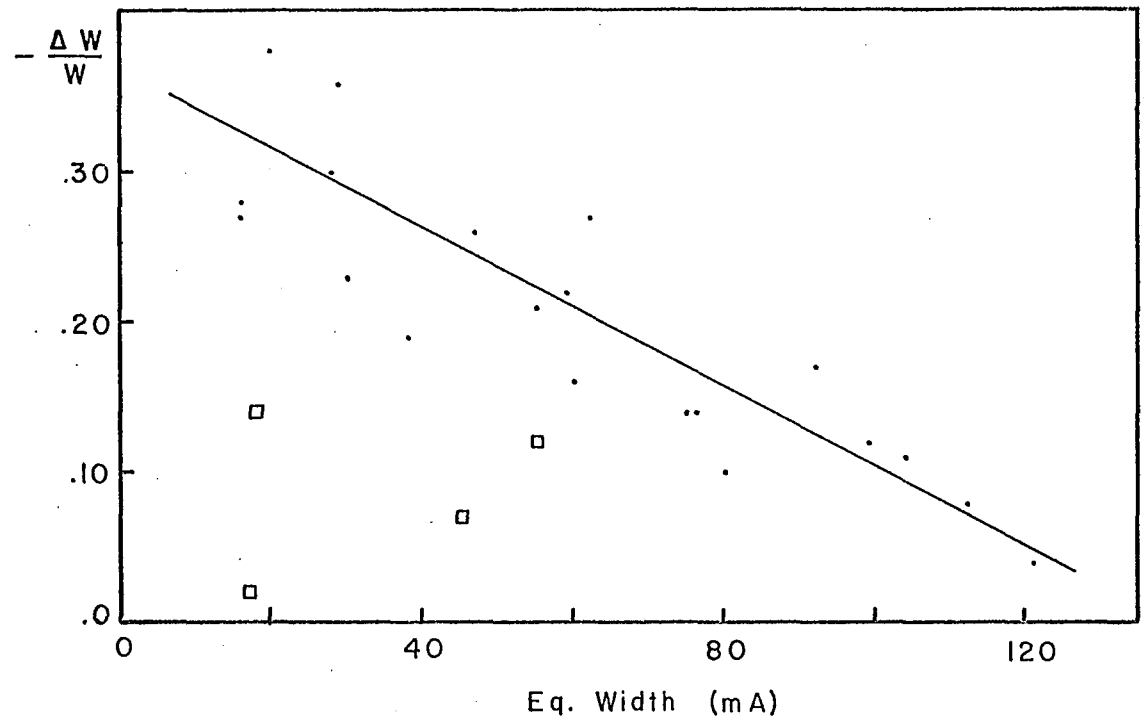


Fig. 22. Fractional Changes in Equivalent Width

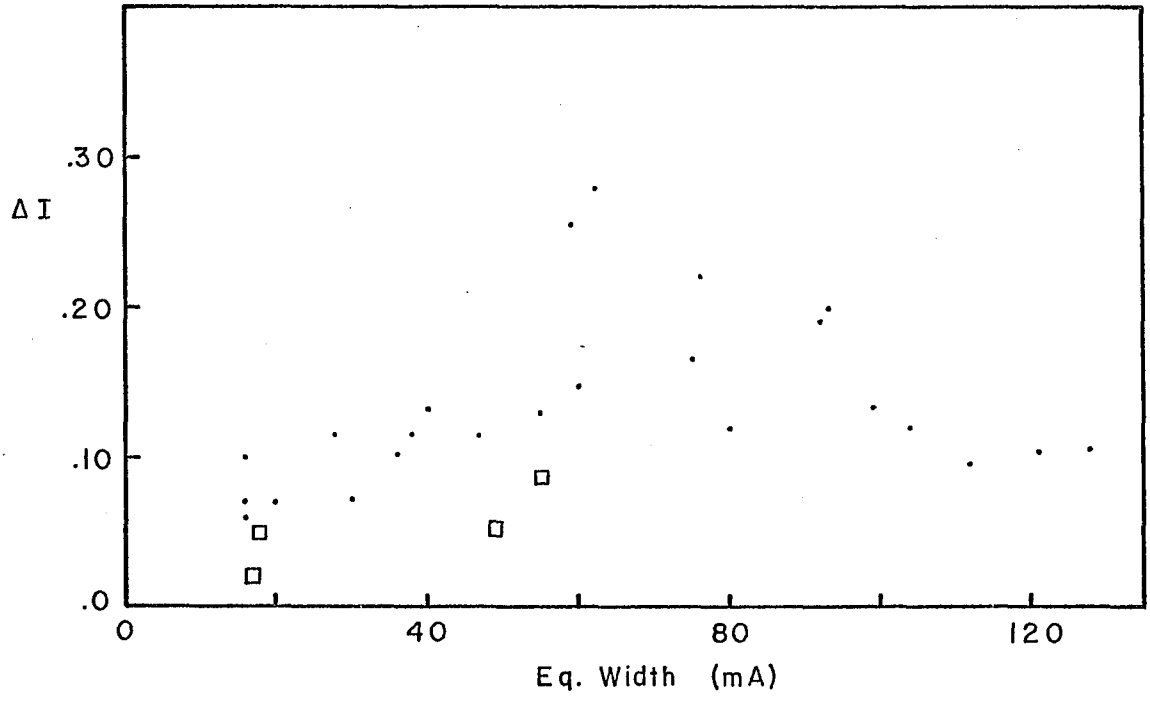


Fig. 23. Fractional Changes in Central Intensity

demonstrated that for most neutral lines, non-Zeeman effects are dominant. Figure 23 shows that for lines of large equivalent width the change in central intensity is similar to or less than that for lines of low to intermediate equivalent width. Also for the range between approximately 60-100 mA, there seems to be a trend toward higher values of $\Delta I/I_c$. This evidence suggests that weakening effects for photospheric lines may be greater for those of moderate strength.

Preliminary study of spectroheliograms in such "gap-sensitive" lines as λ6302.5 (Fe I) do not show weakenings close to the limb nearly as well as they do in the vicinity of the disk center.

Such preliminary evidence suggests that for photospheric lines, the weakening effect decreases above the usual region where the center of the λ6302.5 line is formed near the center of the solar disk.

d. Effects of Excitation Level. We might expect that since lines of ions show appreciably less weakening than lines of neutral atoms, then lines of neutral atoms arising from the higher energy levels ought to be weakened less than lines arising from lower levels. The dependence

of the weakening, $\Delta I$, (in units of the continuum), versus excitation potential (E.P.) is shown in Figure 24 for the lines on spectrogram 2, July 4, 1966 (Table 7). Figure 25 shows $-\Delta W$ versus E.P. for the same spectrogram. The lines of higher excitation potential tend to have lower values of $\Delta I$ and lower values of $-\Delta W$, indicating that the lines originating from lower energy levels are weakened more than lines originating from higher energy levels. Four lines of ions (shown by squares) all lie near the bottom of the graph as would be expected from earlier discussion.

An empirical indication of the effects of excitation conditions in a "field-region" can be obtained from the apparent change in strength of a line in a sunspot. The apparent change is indicated by a letter in the Rowland Tables. The letters and their meaning in terms of a sunspot's effect on the strength of the line are:

W - the line is greatly weakened
w - the line is weakened
u - the line is unchanged
s - the line is strengthened
S - the line is greatly strengthened

One would expect, then, that if the excitation conditions in a photospheric "field-region" are higher than in the undisturbed photosphere, that the effects on a line would be

Figure 24. Fractional Changes in Central Intensity versus the Excitation Potential of the Lower Level, Spectrogram 2, July 4, 1966

Lines arising from lower levels having higher potential (E.P.) tend to have smaller changes in central intensity, $\Delta I$, (in units of the continuum) than lines arising from levels having lower excitation potentials. The squares represent lines of ions.

Figure 25. Decrease in Equivalent Width versus the Excitation Potential of the Lower Level, Spectrogram 2, July 4, 1966

Lines arising from lower levels having higher excitation potential (E.P.) tend to have smaller decreases in equivalent width ($-\Delta W$) than lines arising from levels having lower excitation potentials. The lines of ions are represented by squares.

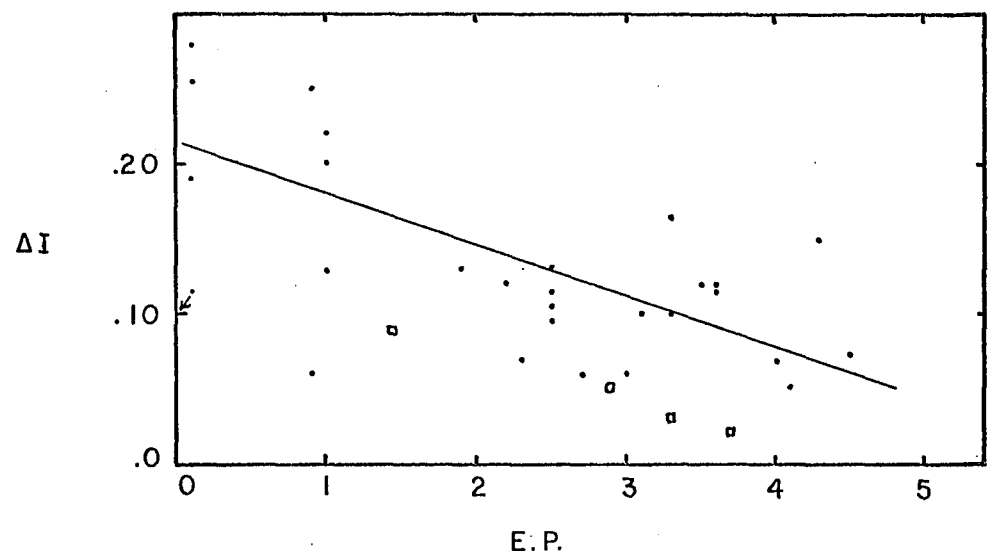


Fig. 24. Fractional Changes in Central Intensity

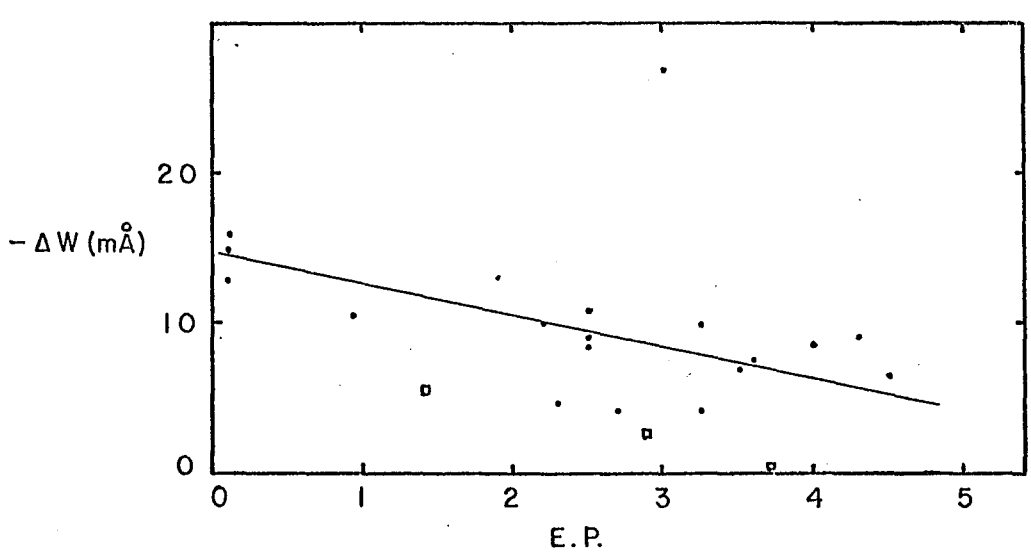


Fig. 25. Decrease in Equivalent Width

the reverse of those given here for sunspots since sunspots are known to be cooler than the normal photosphere. Figure 26 shows that, for spectrogram 2 of July 4, 1966, the w-lines are weakened least and the S-lines are weakened most in the "gaps". Therefore, it seems that the excitation conditions in a photospheric field region are higher than in the surrounding field-free photosphere.

Figure 26. Fractional Changes in Central Intensity versus Sunspot Classification for lines of Spectrogram 2, July 4, 1966

Lines that weaken most (w-designation) in sunspots have smaller increases in central intensity than lines that strengthen most (S-designation) in sunspots. The squares represent lines of ions.

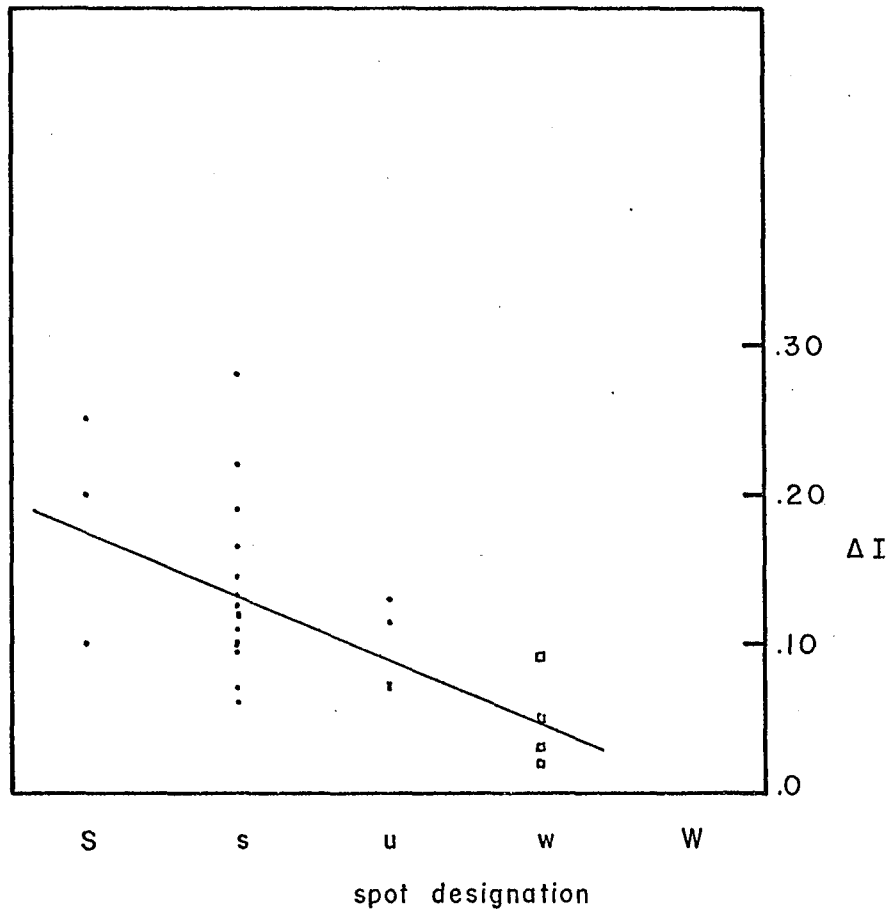


Fig. 26. Fractional Changes in Central Intensity

# IV. DISCUSSION

## A. Physical Conditions in Magnetic-Field Regions

Small regions of relatively strong magnetic field have been found in which lines of neutral elements are weakened. The weakening of lines such as λ5250.2 of Fe I can correspond to an increase in central intensity of as much as $\Delta I/I \approx 95\%$ and a decrease in equivalent width of as much as $\Delta W/W \approx 27\%$. For other lines of high Zeeman sensitivity, $\Delta I/I$ may reach 60% and $-\Delta W/W$ may reach 10-14%. The values determined for $\Delta I/I$ and $\Delta W/W$ depend not only on the line in question but also very much on the quality of seeing. Determining the amount of $\Delta I/I$ due to Zeeman splitting requires fairly accurate knowledge of the strength of the magnetic field associated with the weakening. For λ5250.2 the direct contribution of non-Zeeman effects is about 70% of the observed total $\Delta I/I$. For most of the other neutral lines studied, the major contribution to $\Delta I/I$ still appears to come from non-Zeeman effects (arising from different physical conditions in the magnetic field regions than elsewhere).

We will now try to determine in what way the physical conditions are different in the field regions than in the non-field regions. Probably the most significant general result concerning non-Zeeman effects is that, in field regions, the lines of ionized atoms are weakened appreciably less than the lines of neutral atoms, indicating that the abundance ratio of neutral atoms to singly-ionized atoms is smaller in these regions than that in field-free regions. This increase in the degree of ionization suggests that the temperature is higher in the magnetic field regions.

A crude idea of the difference in temperature between field and non-field regions might be obtained by using the Planck function to convert changes in $I_\nu$ into changes in temperature assuming $I_\nu = B_\nu$. For all lines between about 50 and 130 mA in equivalent width form Spectrogram 2, July 4, 1966 (Table 7), the average $\Delta I/I$ is 0.52 including Zeeman effects which are, however, small compared to the total $\Delta I/I$. Assuming that the centers of these lines represent a temperature of $4700^{\circ}K$ ($\tau \approx 0.02$, Bilderberg Continuum Atmosphere, Gingerich and de Jager, 1968), then from $I_{field}/I_{non\text{-}field} = 1.52$ we obtain, using $I_\nu = B_\nu$,

$\Delta T \approx 360^{o}K$ between the regions of line formation in the field and outside the field. However, the application of the Planck function in such a simple way may not be reliable. Furthermore, the observed $\Delta I/I$ and hence the inferred $\Delta T$ may not refer to the same physical height in the solar atmosphere since the line absorption coefficient in the field region is probably different from that outside the field.

The temperature difference can also be found by assuming LTE and, through the use of the Saha and Boltzmann equations, determining the change in temperature associated with the magnetic field from measured abundance changes in the atomic level giving rise to the line in question. The changes in atomic abundances have been determined from changes in equivalent width of weak lines (<30 mA), assuming that changes in their equivalent width are directly proportional to changes in abundance. Since the effects of changes in partition functions and electron density are not large compared to the effect of changes in temperature, the partition functions and the electron density are assumed to be unchanged in a magnetic field region. Use of this procedure with the data on weak lines in Table 7, gives a temperature difference of $160^{o}K$ between field and non-field regions.

This temperature difference is somewhat lower than the previous one but the two determinations indicate a value in the vicinity of a few hundred degrees K.

Since even very weak Fraunhofer lines (W $\approx$ 10-20 mA) are weakened in field regions, it would be interesting to know how far down in the atmosphere the physical conditions are altered. Recently, Bonnet and Blamont (1968) have obtained spectroheliograms in the UV-continuum at 2235 A and 1980 A showing brighter-than-average regions (with higher contrast at $\lambda$1980) on the solar disk in the same places as Ca II K emission. Since K emission is correlated with the position of magnetic field regions on a large scale, these bright regions in the UV must correspond to magnetic field regions. An approximate idea of the height of these UV bright regions can be obtained from the contribution functions for these two wavelengths if we assume that the emission from field regions is formed at about the same height as the field-free continuum. These functions, given by Bonnet and Blamont, reach a peak at about $\tau_{5000} = 0.1$ for $\lambda$2235 and $\tau_{5000} = 0.005$ for $\lambda$1980. Referring to the Bilderberg model, these optical depths correspond to heights above the photosphere of about 124 and 300 km, respectively.

It is very probable that white-light faculae, seen near the limb of the sun ($\cos\theta \lesssim 0.6$) correspond to the photospheric magnetic fields associated with the weakening of Fraunhofer lines. A number of studies of white-light faculae have indicated that they have higher temperatures than the surrounding field-free photosphere. For example, using curves of growth, Mitropol'skaya (1952) found $\Delta T \approx 200^{o}K$, and more recently Voikhanskaya (1966) found $\Delta T \approx 200$-$300^{o}K$. Rogerson (1961) measured the contrast of faculae very close to the limb ($\cos\theta \approx .14$) appearing on Stratoscope pictures. For these features he found $\Delta I/I \approx 0.63$ and interpreted this as a temperature increase of approximately $900^{o}K$ over that of the surrounding photosphere, based on a rather crude model of a facula. However, if faculae have a greater optical depth than Rogerson assumed, their inferred temperature difference would be less than $900^{o}K$. If the faculae were approximately homogeneous and had a large optical depth, then one might have $I_{\nu} \approx B_{\nu}$ and, applying the $\Delta I/I$ of 0.63 observed by Rogerson to the Planck function, the temperature difference could be as low as about $300^{o}K$. This value of $300^{o}K$ may be more plausible since the Bilderberg model shows that a horizontal path-length of 700 km (the size of

faculae assumed by Rogerson), at a height where the faculae are formed ($\tau_{5000} \approx .1$-$.3$), has an optical depth of $\approx$ 1-4. If white-light faculae do correspond to magnetic field regions, then the temperature difference for faculae suggests that photospheric magnetic field regions are probably several hundred degrees K hotter than the surrounding photosphere. The temperature difference inferred earlier from the mean $\Delta I/I$ of Fraunhofer lines is thus roughly consistent with the temperature difference suggested by the white-light faculae. Moreover, since the white-light faculae become visible at approximately $\cos \theta \simeq .6$, which corresponds to $\tau_{5000} \approx .6$, the temperature in a field region begins to be higher than that of the surrounding atmosphere slightly above the photosphere (roughly 30-40 km, according to the Bilderberg model). However, these arguments still leave much uncertainty in the temperature difference determined for the photospheric line weakenings because the Fraunhofer lines used may be formed at different heights than the white-light faculae.

If one could study line weakenings near the center of the solar disk in continuum radiation, it would be easier to interpret the observations. Since magnetic field regions appear as locally-bright regions in the UV continuum and

near the limb in white-light, one would also expect to see them as brighter-than-average features in the far infrared continuum (5-10$\mu$), which is formed above the visible photosphere at $\tau_{5000} \approx .1\text{-}.2$, according to the Bilderberg model.

## B. Ca II Network

In the past, the Ca II chromospheric network has been used to locate magnetic fields in the photosphere. However, we have now found that the Ca II network is only approximately correlated in position with photospheric magnetic fields. The lack of complete spatial correlation is not due to poor resolution. Figures 2 and 3 have shown that the chromospheric network is larger and more extensive than the photospheric network. In Figure 3 the photospheric network is taken to be that shown in the wings of Ca I $\lambda$4227. We have already seen that the photospheric network is exactly cospatial with the photospheric magnetic fields. The most obvious question that arises is whether or not the Ca II chromospheric network is correlated with magnetic fields in the chromosphere. If there is a field in the chromosphere wherever Ca II emission appears, then the field must diverge considerably in some places as it reaches from the photosphere into the chromosphere. On the other hand,

there may be regions of Ca II emission containing no magnetic field but receiving energy from nearby regions which do contain magnetic fields. Thus, the relationship of Ca II emission and magnetic fields needs further study. A direct way of investigating the relationship would be to measure the magnetic fields in the chromosphere to determine if the Ca II $K_{232}$ emission is cospatial with magnetic fields.

## C. Magnetograph Calibration

We have seen how the shape of Fraunhofer lines can be altered in a magnetic field due primarily to changes in the physical conditions of the atmosphere. An implication of this change in shape is that the calibration of magnetographs can not properly be obtained from the "average" photosphere but, in principle, should be obtained for each magnetic region observed. It does not seem practical to obtain a calibration for every feature, but it may be possible to apply an average correction factor to the calibration determined from the average photosphere. Since the slope of the intensity profile is decreased in the field region, the Babcock-type and the Leighton-type magnetographs are affected since they usually assume that the slope of the line being used is the same for a field region as for the "average"

photosphere. This assumption may result in underestimating the "true" field strengths by as much as a factor of about 2. Specifically, for $\lambda$5250.2, commonly used in photoelectric magnetographs, the slope of the linear portion of the line decreased by a factor of 1.74 in a strong "gap."

## D. Future Work

The dependence of the change of physical conditions on height in the solar atmosphere has not been well determined in this study. We have seen that in the continuum forming region of the atmosphere, there is often no difference between the intensity in the field region and the intensity in non-field regions. In fact there is often a lower intensity in the field region than elsewhere in the continuum-forming layers. In the regions where weak to moderately strong Fraunhofer lines are formed, the temperature is higher in the field region than outside, showing that the temperature difference between field and non-field regions must increase with height in some fashion. The rate of increase has not been determined, however.

One method of pursuing the effect of height would be to investigate the weakening of Fraunhofer lines as a function of position on the disk, $\theta$. Since one would then have

to look at different regions, one could get only statistical evidence about the variation with height. Another method of obtaining height variation would be to observe the strength of weakenings as a function of wavelength in the far infrared continuum. This latter method would allow one to study the height variation of the same features and, since the observations are of continuous radiation, they should be easier to interpret in terms of physical conditions in the solar atmosphere then observations of Fraunhofer line radiation. Observations at various wavelengths in the UV continuum could also be used to determine variation with height, but these observations would be more difficult to carry out due to line crowding in the UV and the need to use balloon or satellite observing stations in order to reduce atmospheric absorption.

An area of observation that could be fruitful using balloon observations is that of determining the true two-dimensional size and shape of the small magnetic field regions and their location in the granulation pattern. Beckers and Schröter (1966) found that the small fields observed by them were located in intergranular spaces where the continuum intensity was 10-12% less than the surrounding

photosphere. However, the "gap" of spectrogram 2, July 4, 1966 (see Table 7) had a measured continuum intensity only 2 or 3% less than that of the surrounding photosphere, thus raising the question of whether or not this gap was located in a "normal" intergranular space. Furthermore, with higher spatial resolution, the regions of magnetic field might be smaller than now thought, a result that if true, would imply that these magnetic fields have greater field strengths than those measured from the ground.

Temporal-spatial studies of weakenings would be interesting for two reasons. First, by studying the change in position of weakenings with time, one can determine the motions of photospheric magnetic fields. Second, by studying the strength of weakenings as a function of field strength and time, we can perhaps learn something about the energy source that alters the physical conditions in the magnetic field regions. If it is found that the strength of the magnetic field does not change rapidly compared to possible changes in the strength of the weakening, then any time changes in the strength of the weakening will be almost entirely a result of energy gains and losses within the field region. Possible energy sources might be supergranular or

granular motions or perhaps some less organized form of energy. We have seen (Figure 4) that the velocity-granulation is modified in magnetic field regions. Perhaps some of the kinetic or thermal energy usually present in the granulation is channeled into the magnetic field regions thereby heating the atmosphere and causing the observed weakening of Fraunhofer lines.

## V. SUMMARY

The major results of this study are summarized below:

A. Photospheric weakenings (or gaps) are exactly cospatial with line-of-sight magnetic fields in the photosphere seen on Z-photos. These magnetic fields have typical strengths of several hundred gauss and sometimes reach strengths of about 500 gauss. Magnetic fields of 200-300 gauss have been found with linear sizes of less than 800 km. Although no evidence was found for non-spot field strengths of 1000-1200 gauss given by Beckers and Schröter (1966), with improved calibration of Z-photos, field strengths of up to 600-700 gauss might be measured.

B. Photospheric line weakenings form a delicate photospheric network similar to, but much finer than, the familiar chromospheric K-line network. The wings of very strong lines also show the photospheric network, whereas the cores of very strong lines show a diffuse network resembling the chromospheric K network. Therefore, the chromospheric network (particularly that of the Ca II K-line) is not exactly cospatial with photospheric magnetic fields. The contrast

of the photospheric network is typically about 30%, whereas that of the Ca II K-line is much higher.

D. Most of the weakening of Fraunhofer lines of neutral elements is not due to Zeeman splitting, but is due to a difference in the physical conditions between the field and non-field line-forming regions of the solar atmosphere. The alteration of the physical conditions is such that neutral lines are weakened more than ionized lines and among neutral lines, those arising from low-lying levels tend to be weakened more than those arising from higher levels.

In conclusion, it is suggested that the weakening of Fraunhofer lines is largely due to an increase in temperature of several hundred degrees, in magnetic field regions, relative to that of the surrounding field-free photosphere. This rise in temperature first becomes appreciable perhaps some 30-40 km above the $\tau_{5000} = 1$ level in the photosphere and can be seen as white-light faculae near the limb. The temperature (and perhaps a density) difference continues on through the line-forming regions, where the photospheric lines are formed, into the chromosphere, where the differences between field and non-field regions seem to become even greater than in the photosphere.

## REFERENCES


Aller, L.H., 1963, Astrophysics: The Atmospheres of the Sun and Stars, 2nd Ed. (New York: Ronald Press Co.).

Ambartsumyan, V.A., 1958, Theoretical Astrophysics (London: Pergamon Press, Ltd.).

Babcock, H.W., 1953, Ap. J. 118, 387.

Beckers, J.M., and Schröter, E.H., 1966, Paper presented at A.A.S. Meeting, Boulder, Colo.

Bonnet, R.M., and Blamont, J.E., 1968, Solar Physics 3, 64.

Chapman, G.A., and Sheeley, N.R., Jr., 1967, I.A.U. Symposium 35, Budapest. (in press)

Gingerich, O., and deJager, C., 1968, Solar Physics 3, 5.

Hale, G.E., 1908, Ap. J. 28, 315.

Hale, G.E., 1922, Pub. Astron. Soc. Pacific 34, 59.

Harvey, J. and Sheeley, N.R., Jr., 1965 (unpublished).

Howard, R., 1967, Annual Review of Ast. and Ap., Vol. 5 (Palo Alto: Annual Reviews, Inc.).

Leighton, R.B., 1959, Ap. J. 130, 366.

Minnaert, M. Mulders, G.F.W., and Houtgast, J. 1940, Photometric Atlas of the Solar Spectrum (Utrecht).

Mitropol'skaya, O.N., 1952, I.K.A.O., 8, 93.

Moore, C.E., 1945, Multiplet Table, Revised (Princeton University Press).

Moore, C.E., Minnaert, M.G.J., and Houtgast, J., The Solar Spectrum 2935A to 8770A, NBS Monograph 61, 1966.

Rogerson, J.B., 1961, Ap.J., 134, 331.

Seares, F.H., 1920, Observatory, 43, 310.

Sheeley, N.R., Jr., 1964, Thesis, Cal. Inst. Tech.

Sheeley, N.R., Jr., 1966, Ap.J., 144, 723.

Sheeley, N.R., Jr., 1967, Solar Physics, 1, 171.

Tanberg-Hanssen, E., 1967, Solar Activity (Waltham: Blaisdell Publishing Co.).

Voikhanskaya, N.F., 1966, Sov. Ast., 10, 325.

Waldmeier, M., 1949, Z. f. Ap., 26, 147.

White, H.E., 1934, Introduction to Atomic Spectra (New York: McGraw Hill Co.).